Title
Mechanisms, Regulation and Function of Synaptic Plasticity in the Striatum

Author
Lerner, Talia Newcombe

Publication Date
2011

Peer reviewed|Thesis/dissertation

Mechanisms, Regulation and Function of Synaptic Plasticity in the Striatum

by

Talia Newcombe Lerner

DISSERTATION

Submitted in partial satisfaction of the requirements for the degree of

DOCTOR OF PHILOSOPHY

in

Neuroscience

in the

GRADUATE DIVISION

of the

UNIVERSITY OF CALIFORNIA, SAN FRANCISCO

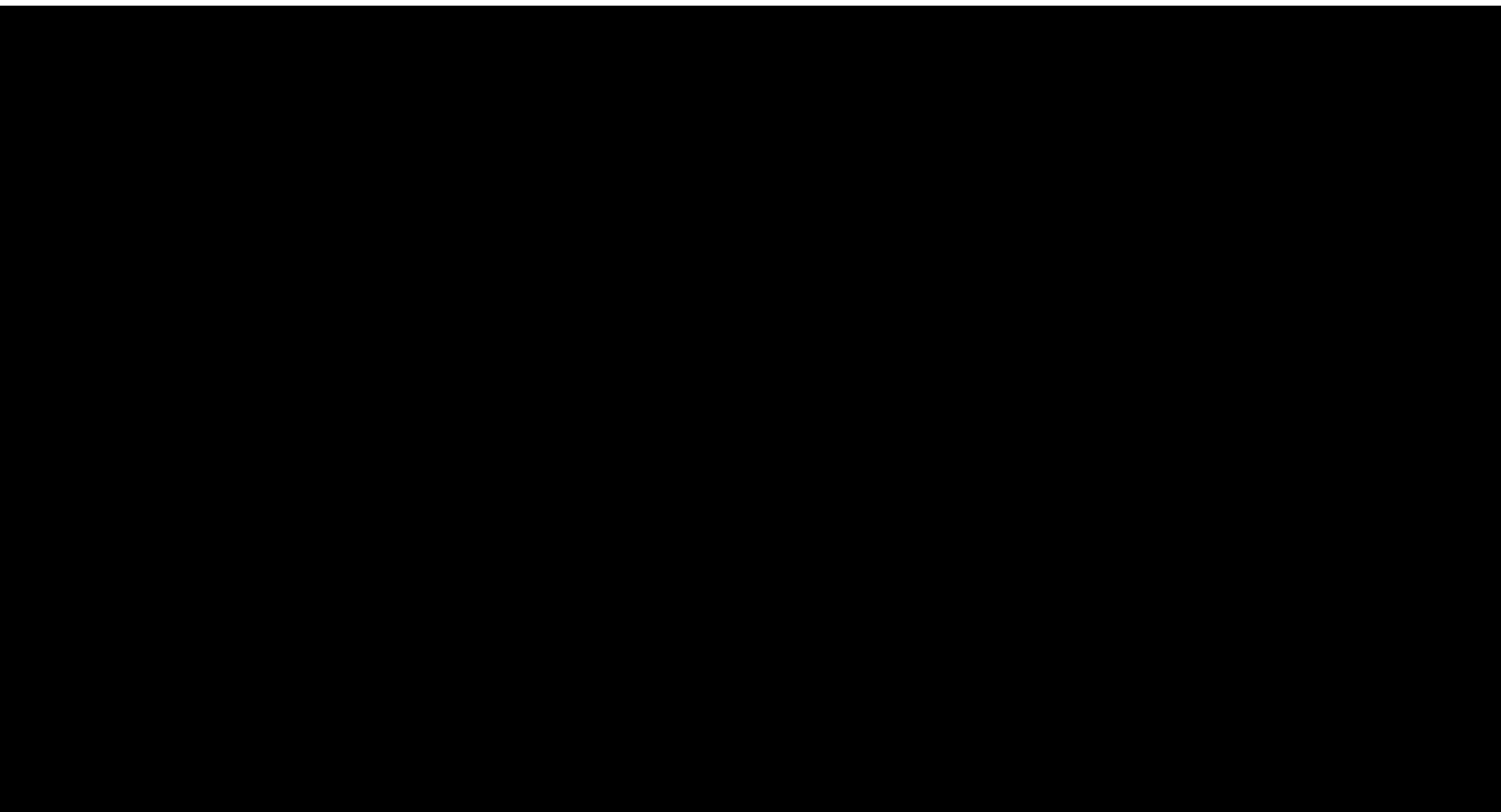

In loving memory of my grandmother, Hanna Newcombe,

activist, scholar, and eternal inspiration

Acknowledgements

This thesis is the end product of a complex personal journey through graduate school. When I arrived at UCSF in the fall of 2006, I was passionate, but also timid, unsure and undeveloped as a scientist. I have many, many people to thank for seeing my potential and helping me to develop into the scientist and the person that I am today.

First and foremost, I need to thank my family – my mother, Nora Newcombe, my father, Jeffrey Lerner, and my brother, Andrew Lerner – for their wisdom, guidance and support. My family pushes me everyday to be a better person and believes in me even when my own confidence wavers. I'm lucky to have been brought up by such thoughtful people, who provided a home where curiosity was the highest of virtues.

I also need to thank my husband, John Sanders, who always keeps me on my toes. John was there to see me through my highest highs and lowest lows. He knows me better than anyone else in the world and loves me "warts and all."

In addition to John, my best friend, I thank all the great friends who have sustained me throughout graduate school. When I needed to complain, they listened to me. When I needed to forget, they distracted me. When I needed to daydream, they indulged me. When I needed to focus on my work, they understood. My smart, talented friends challenge me constantly and make me think in new and different ways. Thank you. I could not have made it through graduate school without you.

I would also like to thank the many UCSF faculty members who have taught me and advised me. Almost all of the faculty members in the Neuroscience Program have helped me in some way during my time here. In particular, Patricia Janak, my faculty advisor when I entered graduate school and my qualifying exam committee chair, was and is forever patient and kind. Cynthia Kenyon, my first quarter rotation advisor,

encouraged me tremendously and made me feel welcome in graduate school. Louis Reichardt, the head of the Neuroscience program, advised me when I was lost after my third rotation and was nervously trying to find a thesis advisor. My thesis committee members, Roger Nicoll, Antonello Bonci, Robert Edwards and Steve Finkbeiner, have each been instrumental in helping me to develop my thesis project. I am especially thankful to Roger for helpful advice on finding a postdoctoral position and to Anto for always having thoughtful comments for me on all aspects of being a scientist. I also thank John Huguenard of Stanford for kindly serving as the “outside” member of my thesis committee at my thesis defense.

This thesis would not have been possible without the help of Patricia Veitch, the Neuroscience Program coordinator, and Carrie Huckaba and Lucita Nacionales, the former and current Neuroscience Program assistants. Their hard work everyday ensures the program runs smoothly. Every time I stopped by the office with a problem, they were eager to help. I am amazed at how, with so many students going through the program, Pat, Carrie and Lucita seem to care about each and every one, an accomplishment worth recognizing.

Finally, I owe a huge debt of gratitude to Anatol Kreitzer, my thesis advisor. He accepted me into his lab in the summer of 2007 when I was lost, unsure and untrained. He literally sat next to me for days teaching me to patch. He believed in me. He trusted me. He never seemed to doubt that my fumbling attempts at experiments could eventually become papers and a thesis project. Without him, more than any single person, I would not be the scientist I am today. I’m consistently impressed by Anatol’s fearless style of doing science and his unique talent for identifying important and interesting, but readily addressable questions. During my time in the lab, it has grown from essentially nothing to a vibrant group of ten people. It has been incredible to watch this development. I feel so lucky to have had the opportunity to observe and learn from

Anatol and all the excellent scientists he has recruited to the lab. I don't think I have to say (but I will anyway) that I already thanked the members of the Kreitzer Lab when I thanked my friends. It has been a pleasure to work with all of you. I'm proud and privileged to be a Kreitzer Lab alumna.

Author Contributions

The text of Chapter 2 of this thesis is a reprint of the material as it originally appeared in the Journal of Neuroscience (Lerner et al., 2010). Talia Lerner performed all the behavior and electrophysiology experiments in this chapter. Eric Horne, the second author on the publication, performed the mass spectrometry experiments. Nephi Stella and Anatol Kreitzer, the third and senior authors on the publication, respectively, directed and supervised the research. Talia Lerner and Anatol Kreitzer co-wrote the paper.

The text of Chapter 3 of this thesis is a preliminary version of a manuscript that will appear in Neuron (in press). Talia Lerner performed all the experiments in this chapter. Anatol Kreitzer, the co-author on this publication, directed and supervised the research. Talia Lerner and Anatol Kreitzer co-wrote the paper.

Some of the text of Chapters 1 and 4 of this thesis (Introduction and Conclusion) is a reprint of the material that originally appeared in Current Opinion in Neurobiology (Lerner and Kreitzer, 2011). Talia Lerner and Anatol Kreitzer co-wrote this review article.

Abstract

The basal ganglia are a network of subcortical brain nuclei important for action selection and motor learning. Excitatory synapses onto projection neurons in the striatum, the input nucleus of the basal ganglia, are a major site of long-term synaptic plasticity. This plasticity has the potential to powerfully regulate motor function by setting the gain on the incoming cortical signals that drive basal ganglia circuits. Endocannabinoid-dependent long-term depression (eCB-LTD) is the best characterized form of striatal plasticity, but the mechanisms governing its normal regulation and pathological dysregulation are not well understood. This thesis examines the molecular mechanisms underlying striatal eCB-LTD. It focuses on eCB-LTD at excitatory synapses onto a subset of striatal projection neurons, or medium spiny neurons (MSNs), the "indirect-pathway" MSNs. These MSNs express dopamine D2 and adenosine A2A receptors and project to the external segment of the globus pallidus. In this thesis, I characterize two distinct biochemical signaling pathways mediating eCB production in striatal indirect-pathway MSNs: a PLCβ- and DAG lipase-dependent pathway that is engaged by low-frequency stimulation, and a novel Src- and PLD-dependent pathway that is engaged by high-frequency stimulation. Endocannabinoid production through both signaling pathways is modulated by dopamine D2 and adenosine A2A receptors, acting through cAMP/PKA. I identify Regulator of G-protein Signaling 4 (RGS4) as a key link between D2/A2A signaling and eCB mobilization pathways. Behaviorally, I find that indirect-pathway eCB-LTD likely underlies at least some of the stimulant properties of A2A receptor antagonists and that the loss of indirect-pathway eCB-LTD may mediate the development of parkinsonian motor deficits following dopamine depletion. In experiments using RGS4 knockout mice, which in contrast to wildtype mice exhibit normal eCB-LTD following dopamine depletion, I show that the loss of RGS4 leads to

fewer behavioral deficits after dopamine depletion, suggesting that inhibition of RGS4 may be an effective non-dopaminergic strategy for treating Parkinson's disease.

TABLE OF CONTENTS

LIST OF TABLES AND FIGURES

Chapter 1

Chapter 2

Chapter 3

CHAPTER 1

Introduction

The brain is the organ that defines us. It imbues us with consciousness, it stores our memories, it defines our personalities, and we use it to control almost everything we do. Neuroscience, the study of the brain, is about figuring out what it is about this three pound lump of flesh that allows it to serve such incredible, complex functions. While we are still far from understanding everything about the brain, much has been figured out since Santiago Ramon y Cajal first postulated the “neuron doctrine” in 1891. One of the greatest advances has come from the understanding that the brain is not a fixed structure. It is capable of a huge amount of change and adaptation in response to our experience. Even adults, whose brains are less plastic than children’s, learn and remember new things constantly. To do so, *something* about their brains must change.

What is the neural basis of learning? A great deal of evidence has accumulated that activity-dependent alterations in the strength of synaptic connections between neurons mediate learning. Which synapses change (and where, why, when and how) is still a subject of active study and the answers depend heavily on what is being learned or experienced. For example, if you memorized a fact, such as the width of the major groove of B-form DNA, or formed a spatial memory, such as how to get to the room your biochemistry class is being held in, you probably experienced synaptic plasticity in your hippocampus. However, if you learned a motor skill, such as how to how to touch type, or you acquired a habit, such as turning off the light every time you leave your bedroom, or you automated a routine, such as navigating to that biochemistry classroom, so that it no longer requires conscious effort, you probably experienced synaptic plasticity in your striatum. This thesis focuses on understanding the molecular mechanisms of synaptic

plasticity in the striatum in the hopes of better understanding how this process is connected to learning as well as to diseases, such as Parkinson's disease, in which aberrant learning-like processes may take place.

The Striatum, the Basal Ganglia, and Motor Function

The striatum is the input nucleus for a network of subcortical brain nuclei known as the basal ganglia. Inputs to the striatum, from the cortex and thalamus, are processed in two parallel pathways within the basal ganglia – the direct and the indirect pathways – which diverge from the striatum and converge again in the basal ganglia's output nuclei, the substantia pars reticulata and the internal segment of the globus pallidus (Fig.1).

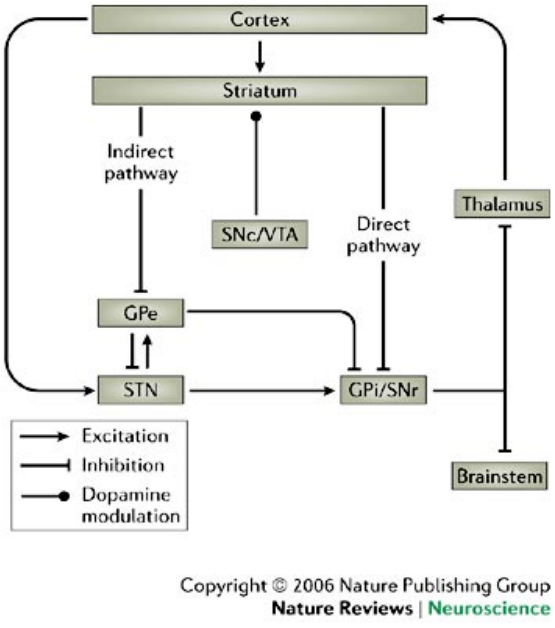

Figure 1. Basal Ganglia Circuitry. The direct and indirect pathways diverge from the striatum and exert opposite effects on downstream activity in the substantia nigra pars reticulata and the internal segment of the globus pallidus. STN, subthalamic nucleus; GPe, external segment of the globus pallidus; GPi, internal segment of the globus pallidus; SNr, substantia nigra pars reticulta; SNc, substantia nigra pars compacta; VTA, ventral tegmental area. (adapted from (Graybiel et al., 1994; Hikosaka et al., 2000; Yin and Knowlton, 2006)

What does information flowing through these two parallel pathways in the basal ganglia do? As alluded to above, the basal ganglia are thought be important for motor learning and habit formation, however the precise role of the basal ganglia in various

aspects of motor function is still being debated. The basal ganglia have also been postulated to be important for many other motor functions such as action selection, movement initiation, online motor error correction and controlling the scaling of movement (for review, see Packard and Knowlton, 2002; Turner and Desmurget, 2010; Yin and Knowlton, 2006).

The simplest model of basal ganglia circuit function, which, despite its shortcomings, has dominated much of the thinking in the field, is the Albin-DeLong model, based on the clinical manifestations of Parkinson's and Huntington's Diseases. According to this model, increased activity of the direct pathway facilitates movement, whereas increased activity of the indirect pathway inhibits movement. While this is an oversimplification of the complex basal ganglia circuit (for review see (DeLong and Wichmann, 2009)), recent tests of the model have lent support to its general structure. Using viral-mediated cell-type-specific expression of channelrhodopsin-2, our lab demonstrated that firing rates of direct- and indirect-pathway medium spiny neurons (MSNs), the projection neurons of the striatum, control different aspects of movement in the directions predicted by the Albin-DeLong model (Kravitz et al., 2010). Further evidence for this hypothesis comes from experiments that selectively lesioned indirect-pathway MSNs, a manipulation that led to dramatic increases in locomotor behavior (Durieux et al., 2009).

Direct- and Indirect-Pathway Medium Spiny Neurons Are Distinct

The striatum is made up largely of GABAergic projection neurons, called medium spiny neurons (MSNs). About half of the MSNs are part of the "direct pathway" and half belong to the "indirect pathway." Although MSNs were once thought to be a mostly homogenous population of neurons, it has become evident in the past 5-10 years that MSNs of the direct and indirect pathways differ significantly in a number of respects

aside from their projection targets. Direct-pathway MSNs express dopamine D1 receptors, muscarinic acetylcholine M4 receptors, substance P and dynorphin, while indirect-pathway MSNs express dopamine D2 receptors, adenosine A2A receptors, and enkephalin. The differences in receptor expression lead to differences in the regulation of long-term plasticity (discussed in more detail below under "Striatal Plasticity Mechanisms" and throughout this thesis). Indirect-pathway MSNs are more excitable than direct-pathway MSNs and have less elaborate dendritic trees (Day et al., 2008; Gertler et al., 2008; Shen et al., 2007). Differences in synaptic properties, such as larger NMDA/AMPA receptor ratios and higher release probabilities at excitatory synapses onto indirect pathway MSNs, have also been reported (Kreitzer and Malenka, 2007). These differences may be due in large part to differential innervation of direct-pathway and indirect-pathway MSNs by cortical and thalamic axons (Ding et al., 2008). Finally, direct-pathway and indirect-pathway MSNs differ in the extent to which they form lateral inhibitory connections with other MSNs. While indirect-pathway MSNs form synapses onto both direct- and indirect-pathway MSNs, direct-pathway MSNs mostly form synapses onto other direct-pathway MSNs and not onto indirect-pathway MSNs (Taverna et al., 2008). The functional consequences of all of these differences remain to be determined, however, they emphasize the need for the field to think of the two types of MSNs as separate and distinct. BAC transgenic lines that allow easy identification of MSNs of the direct and indirect pathways have been created and will aid in this effort (see "Striatal Plasticity Mechanisms" below for more information). The Drd2-EGFP BAC transgenic line was used extensively in this thesis.

Striatal Plasticity Mechanisms

Given that the firing rates of direct- and indirect-pathway MSNs directly influence movement (Kravitz et al., 2010), it is important to ask what physiological mechanisms

regulate MSN firing rates. In order to fire any spikes at all, MSNs rely on excitatory input from cortex and thalamus (Wilson and Kawaguchi, 1996). Therefore, modulation of excitatory synaptic input strength should be particularly effective at modulating MSN firing rates. Indeed, plasticity at excitatory synapses onto MSNs is involved in motor skill acquisition (Dang et al., 2006; Yin et al., 2009), and is disrupted in animal models of movement disorders, including Parkinson's disease and dystonia (Kitada et al., 2009; Kitada et al., 2007; Kreitzer and Malenka, 2007; Kurz et al., 2010; Peterson et al., 2010; Shen et al., 2008b).

Although synaptic plasticity at excitatory inputs to MSNs has been studied extensively since its discovery in 1992 (Calabresi et al., 1992a), the detailed mechanisms underlying its expression and regulation remain unknown. Fortunately, our understanding of plasticity in the striatum has benefitted greatly from the recent generation and use of BAC transgenic lines that allow easy identification of MSNs of the direct and indirect pathways (Gong et al., 2003; Shuen et al., 2008). The BAC reporter lines rely on the differential expression of G-protein-coupled receptors (GPCRs) in the two types of MSNs: indirect-pathway neurons selectively express G_i-coupled dopamine D2 and G_s-coupled adenosine A2A receptors, whereas direct-pathway neurons selectively express G_i-coupled muscarinic acetylcholine M4 receptors and G_s-coupled dopamine D1 receptors. Thus, fluorescent proteins expressed from the promoters of these receptors selectively label either the indirect or the direct pathway. Differential expression of these G_i and G_s-coupled GPCRs by the two MSN subtypes is not just an experimentally useful coincidence, but reflects important differences in the way that the neuromodulators dopamine, adenosine, and acetylcholine control plasticity in the two pathways. Understanding the molecular mechanisms that regulate LTP and LTD in the striatum is critical because it will allow us to better understand the circuit-level mechanisms that underlie action selection and motor learning by the basal ganglia

circuit. Furthermore, understanding the mechanisms by which dopamine, adenosine, and acetylcholine control striatal plasticity and basal ganglia circuit function will aid the search for new treatments for Parkinson's disease and other basal ganglia disorders.

Indirect-Pathway LTD

In indirect-pathway MSNs, long-term depression (LTD) of excitatory inputs occurs in response to high frequency (100Hz) stimulation paired with postsynaptic depolarization, or in response to negative spike timing (i.e. synaptic stimulation delivered shortly after the MSN spikes) (Ade and Lovinger, 2007; Calabresi et al., 1992a; Fino et al., 2005; Kreitzer and Malenka, 2007; Shen et al., 2008b). The mechanisms underlying indirect-pathway LTD appear to be similar using both protocols. LTD is induced postsynaptically by activation of G_q-coupled mGluRs and L-type calcium channels, which together lead to the mobilization of endocannabinoids (Adermark and Lovinger, 2007; Kreitzer and Malenka, 2005, 2007; Shen et al., 2008b; Sung et al., 2001). Endocannabinoids then travel retrogradely across the synaptic cleft and activate presynaptic CB1 receptors (Gerdeman et al., 2002; Sung et al., 2001). Prolonged activation of CB1 receptors (several minutes) leads to presynaptic expression of LTD as a decrease in release probability (Choi and Lovinger, 1997). Successful induction of indirect-pathway LTD requires activation of dopamine D2 receptors, but also lack of activation of postsynaptic adenosine A2A receptors (Lerner et al., 2010; Shen et al., 2008b). Thus, by regulating the activation of these GPCRs, dopamine and adenosine gate LTD induction in indirect-pathway MSNs.

The most likely downstream mediator of D2 and A2A receptor signaling is cAMP. D2 and A2A receptors are oppositely coupled to cAMP accumulation, just as they are to LTD induction. Additionally, adenylyl cyclase 5 knockout mice have impaired indirect-pathway LTD and the mechanism of LTD impairment is upstream of G_q-coupled mGluRs

(Kheirbek et al., 2009). We do not, however, understand the mechanism of D2 and A2A receptor modulation of LTD downstream of cAMP. Is PKA involved? If so, what are its relevant substrates? This thesis addresses these questions and lays out the convergent signaling cascades of D2, A2A, and mGlu receptors as well as L-type calcium channels.

Indirect-Pathway LTP

Long-term potentiation (LTP) was first observed at excitatory synapses onto MSNs using sharp electrodes and an extracellular solution containing 0 mM Mg^{2+} (Calabresi et al., 1992b). Under these conditions, LTP is induced by high-frequency stimulation. More recently, LTP has been elicited in the presence of physiological Mg^{2+} concentrations using perforated patch recordings and positive spike timing (i.e. synaptic stimulation delivered shortly before the MSN is induced to spike) (Fino et al., 2010; Shen et al., 2008b). LTP is postsynaptically expressed and depends on postsynaptic NMDA receptor activation (Calabresi et al., 1992b; Dang et al., 2006; Flajolet et al., 2008; Shen et al., 2008b). Two recent studies also indicate that the neurotrophic factors FGF and BDNF promote LTP in MSNs, likely through enhancement of NMDA currents (Flajolet et al., 2008; Jia et al., 2010).

In indirect-pathway MSNs specifically, LTP requires A2A receptor activation as well as a lack of activation of D2 receptors, since a D2 agonist can convert the spike-timing dependent LTP into LTD (Flajolet et al., 2008; Shen et al., 2008b). Thus, D2 and A2A receptors gate LTP induction as well as LTD induction. High dopamine levels and low adenosine levels will shift plasticity induction in indirect-pathway MSNs towards LTD. In contrast, low dopamine levels and high adenosine levels will promote LTP in indirect-pathway MSNs.

As with LTD, it is not known how D2 and A2A receptors are able to modulate LTP. However, some clues exist. Since sharp electrodes or perforated patch recordings are required to observe LTP, diffusible signaling molecules are likely involved. Additionally, it was recently shown that D2 and A2A receptors oppositely modulate NMDA receptor signaling through PKA (Higley and Sabatini, 2010). It is not yet clear, however, whether postsynaptic PKA is in fact involved in LTP and, if so, what the relevant substrates of PKA are for this process.

Direct-Pathway LTD

LTD in direct-pathway MSNs is not as well studied as it is in indirect-pathway MSNs, but the literature suggests that its mechanisms, involving postsynaptic G_q-coupled mGluRs and L-type calcium channels and presynaptic CB1 receptors, are similar. LTD in direct-pathway MSNs is blocked by a CB1 receptor antagonist as well as by a G_q-coupled mGluR antagonist (Shen et al., 2008b). Additionally, LTD induced by pharmacological activation of L-type calcium channels has been observed in both direct- and indirect-pathway MSNs (Adermark and Lovinger, 2007).

Although the mechanisms of LTD at excitatory synapses onto direct-pathway MSNs are probably similar to those in indirect-pathway MSNs, the activation of mGluRs and L-type calcium channel signaling, and therefore LTD itself, may be gated by different neuromodulator receptors. Direct-pathway MSNs do not express D2 and A2A receptors, but they do express a complementary pair of G_s- and G_i-coupled receptors: dopamine D1 and acetylcholine M4 receptors (Kreitzer and Malenka, 2008). Using a spike-timing dependent induction protocol, Shen et al. observed LTD in direct-pathway MSNs when D1 receptors were blocked (Shen et al., 2008b). This finding may explain why earlier studies of striatal LTD (Kreitzer and Malenka, 2007) failed to observe LTD at direct-

pathway synapses: if dopamine release is stimulated by an intrastriatal stimulating electrode, this dopamine can activate D1 receptors and block direct-pathway LTD. D1 receptors may thus act similarly to A2A receptors in the indirect pathway, whereas M4 receptors could act similarly to D2 receptors in the indirect pathway. The role of M4 receptors in LTD has not yet been explored experimentally, but M4 is an attractive candidate for a G_i-coupled D2-analog in the direct pathway (Jeon et al., 2010).

Direct-Pathway LTP

The only existing study of LTP in identified direct-pathway MSNs to date showed that LTP can be induced at direct-pathway synapses by positive spike timing using perforated-patch whole-cell recordings (Shen et al., 2008b). This LTP required NMDA receptors, just as it did in indirect-pathway MSNs, but also depended on activation of D1 receptors. An older study using sharp electrodes also found that D1 receptors are required for LTP (Kerr and Wickens, 2001). Thus, in LTP as in LTD, D1 receptors appear to act analogously to A2A receptors in the indirect pathway, implying that cAMP/PKA signaling is likely required to initiate LTP induction in direct-pathway MSNs.

CHAPTER 2

Endocannabinoid signaling mediates psychomotor activation by adenosine A2A antagonists

Abstract

Adenosine A2A receptor antagonists are psychomotor stimulants that also hold therapeutic promise for movement disorders. However, the molecular mechanisms underlying their stimulant properties are not well understood. Here, we show that the robust increase in locomotor activity induced by an A2A antagonist in vivo is greatly attenuated by antagonizing cannabinoid CB1 receptor signaling or by administration to $CB^{-/-}$ mice. To determine the locus of increased endocannabinoid signaling, we measured the amount of anandamide [AEA (N-arachidonoylethanolamine)] and 2-arachidonoylglycerol (2-AG) in brain tissue from striatum and cortex. We find that 2-AG is selectively increased in striatum after acute blockade of A2A receptors, which are highly expressed by striatal indirect-pathway medium spiny neurons (MSNs). Using targeted whole-cell recordings from direct- and indirect-pathway MSNs, we demonstrate that A2A receptor antagonists potentiate 2-AG release and induction of long-term depression at indirect-pathway MSNs, but not direct-pathway MSNs. Together, these data outline a molecular mechanism by which A2A antagonists reduce excitatory synaptic drive on the indirect pathway through CB1 receptor signaling, thus leading to increased psychomotor activation.

Introduction

The basal ganglia and its primary input nucleus, the striatum, are critical for motivation and motor control (Graybiel et al., 1994; Hikosaka et al., 2000; Yin and Knowlton, 2006). The striatum integrates information from the cortex, thalamus, and midbrain, and sends projections to downstream basal ganglia nuclei that regulate thalamocortical motor circuits (Bolam et al., 2000). Striatal projection neurons, known as medium spiny neurons (MSNs), are GABAergic and can be divided into two subclasses based on their axonal projections and gene expression patterns. Direct-pathway MSNs, which project directly to basal ganglia output nuclei, express dopamine D1 receptors. Indirect-pathway MSNs, which project to the globus pallidus, express dopamine D2 and adenosine A2A receptors (Gerfen et al., 1990; Schiffmann et al., 1991; Smith et al., 1998). According to classical basal ganglia models, increased direct-pathway activity facilitates movement, whereas increased indirect-pathway activity inhibits movement (Albin et al., 1989; DeLong, 1990).

A2A receptors are Gs-coupled metabotropic receptors that are highly expressed in the striatum and, to a lesser extent, in other brain regions including the globus pallidus, hippocampus, and cortex (Sebastiao and Ribeiro, 1996). They are enriched in the postsynaptic density of glutamatergic synapses onto striatal indirect-pathway MSNs (Rosin et al., 2003; Schiffmann et al., 2007), although they are also observed in some presynaptic terminals in the striatum and globus pallidus, where they appear to enhance neurotransmitter release (Shindou et al., 2008; Shindou et al., 2003). Behaviorally, A2A receptor agonists decrease movement (Barraco et al., 1993; Hauber and Munkle, 1997) and facilitate the induction of long-term potentiation (Flajolet et al., 2008), suggesting that they increase indirect-pathway activity. In contrast, A2A receptor antagonists increase movement and also cause an increase in immediate-early gene expression in

the globus pallidus, suggesting that they decrease indirect-pathway activity (Hauber et al., 1998; Huang et al., 2005; Mingote et al., 2008; Shen et al., 2008a; Svenningsson et al., 1997). A2A and D2 receptors have opposing effects on cAMP accumulation in indirect-pathway neurons, and inhibition of A2A receptors facilitates D2 receptor-mediated processes (Ferre et al., 1997; Kim and Palmiter, 2008; Stromberg et al., 2000; Tozzi et al., 2007). Because of their actions on the indirect pathway, A2A antagonists have been proposed as an adjunct or alternative to dopamine replacement therapy in patients with Parkinson's disease (PD) (Jenner et al., 2009; Schwarzschild et al., 2006; Simola et al., 2008). However, despite extensive characterization of the intracellular signaling pathways involved in A2A receptor signaling (for review, see Fuxe et al., 2007), little is known about the effector pathways mediating their inhibition of the indirect pathway.

Endocannabinoid signaling is prominent in the striatum and represents a major downstream target of D2 receptor activation in indirect-pathway MSNs (Giuffrida et al., 1999; Kreitzer and Malenka, 2007; Shen et al., 2008b), raising the possibility that it could be influenced by A2A receptors (Rossi et al., 2006). Two major endocannabinoids have been identified thus far: anandamide [N-arachidonoylethanolamine (AEA)] and 2-arachidonoylglycerol (2-AG). These endocannabinoids act as retrograde messengers at synapses, where they are released from postsynaptic dendrites and bind to presynaptic CB1 receptors to depress neurotransmitter release (Chevaleyre et al., 2006; Kano et al., 2009). In the striatum, endocannabinoids underlie both short-term and long-term depression (LTD) of excitatory synapses onto indirect-pathway MSNs (Gerdeman et al., 2002; Narushima et al., 2006a). In this study, we tested the hypothesis that A2A antagonists stimulate motor activity by enhancing endocannabinoid-mediated LTD at striatal glutamatergic indirect-pathway afferents.

Material and Methods

Open-field behavior. Spontaneous locomotor activity was measured in an automated Flex-Field/Open Field Photobeam Activity System (San Diego Instruments). Male wildtype C57BL/6 mice (Charles River) and $CB1^{-/-}$ mice on the C57BL/6 background (Marsicano et al., 2002), aged 7–11 weeks, were used for behavioral testing. Mice were acclimated to the testing room for at least 30 min. Each mouse was injected with 5 μl/g of either N-(piperidin-1-yl)-5-(4-iodophonyl)-1-(2,4-dichlorophenyl)-4-methyl-1H-pyrazole-3-carboxamide (AM251) (5 mg/kg, i.p.) or its vehicle, a solution of 50% polyethylene glycol (PEG) and 50% saline (0.9% NaCl), immediately before being placed in the center of the test chamber. After a 15 min habituation period, baseline locomotor activity was monitored for 15 min. Then, mice were injected with 5 μl/g 2-(2-furanyl)-7-[3-(4-methoxyphenyl)propyl]-7H-pyrazolo[4,3-e][1,2,4]triazolo[1,5-c]pyrimidin-5-amine (SCH442416) (3 mg/ kg, i.p.; also in 50% PEG vehicle) and monitored for another 30 min. Beam breaks were recorded and binned in 3 min intervals. The test chamber was cleaned with 70% ethanol between testing of each mouse. Mice were excluded from analysis if their average number of beam breaks per 3 min period during baseline was <5 or >150 (to eliminate unusually hypoactive or hyperactive mice), or if the SD of baseline values was >80 (to eliminate mice that exhibited highly variable activity). Statistical significance versus baseline within each group was evaluated by a paired t-test. Statistical significance between groups was evaluated by one-way ANOVA with Tukey's honestly significant difference (HSD) test.

Chemical ionization/gas chromatography/mass spectrometry. Mice (C57BL/6; aged 4–5 weeks) were injected intraperitoneally with 5 μl/g of either SCH442416 (3 mg/kg) or its

vehicle (50% PEG). Five to 7 min after injection, mice were killed, and their right and left striatum, as well as their right and left cortex were dissected within 1 min. Each tissue sample (four per mouse) was immediately placed in a 1.5 ml tube, frozen in liquid nitrogen, and stored at -80°C. To reliably quantify the amount of AEA and 2-AG in tissue samples by chemical ionization/gas chromatography/mass spectrometry, three samples of striatum were combined according to each treatment, and their total mass was determined. Because of their larger mass, individual cortical samples were analyzed. All samples were placed in 10 ml of $CHCl_3$ and homogenized for 1 min at 10,000 rpm using a PRO 200 homogenizer (Pro Scientific). The following deuterated standards were added to each homogenate: 150 pmol of d^5-2-AG and 50 pmol of [^{3}H]AEA (Cayman Chemical). Lipids were then extracted, purified, and derivatized as described by Muccioli and Stella (2008). Three microliters of each sample (corresponding to 4–8.5 mg tissue/injection) were then injected by a CP-8400 autosampler into a Varian CP3800 Gas Chromatogram. The temperature elution protocol, chemical ionization parameters, and isotope dilution quantification were as described by Muccioli and Stella (2008). The total ion currents were recorded for each sample and the individual endocannabinoids were identified by their diagnostic peaks (2-AG, 433 m/z; AEA, 330 + 420 + 493 m/z) using MSDATA Review (Varian). Statistical significance was evaluated using a two-tailed unpaired t-test.

Electrophysiology. Coronal brain slices (300 μm) were prepared from Drd2-GFP heterozygotic BAC transgenic mice on the C57BL/6 background (postnatal days 21–35). Slices were superfused with an external solution containing the following (in mM): 125 NaCl, 2.5 KCl, 2 $CaCl_2$, 1 $MgCl_2$, 26 $NaHCO_3$, 1.25 NaH_2PO_4-H_2O, and 12.5 glucose, bubbled with 95% O_2/5% CO_2. Slices were allowed to recover for at least 1 h before recording. Whole-cell voltage-clamp recordings were obtained from visually identified

green fluorescent protein (GFP)-positive or GFP-negative MSNs in dorsolateral striatum at a temperature of 30–32°C, with picrotoxin (50 μM) present to suppress $GABA_A$-mediated currents. Resistance of the patch pipettes was 2.5–4 MΩ when filled with intracellular solution containing the following (in mM): 120 $CsMeSO_3$, 15 CsCl, 8 NaCl, 0.2 EGTA, 10 HEPES, 2 Mg-ATP, 0.3 Na-GTP, 10 TEA (tetraethylammonium), 5 QX-314 (lidocaine N-ethyl bromide), adjusted to pH 7.3 with CsOH. MSNs were held at -70 mV, and excitatory synaptic currents were evoked by intrastriatal microstimulation with a saline-filled glass pipette placed 50–100 μm dorsolateral of the recorded neuron. Test pulses, which consisted of two stimuli 50 ms apart, were given every 20 s. To evoke LTD, MSNs were stimulated at 20 or 100 Hz for 1 s, paired with postsynaptic depolarization to -10 mV. Tetrahydrolipstatin (THL) was purchased from Sigma-Aldrich, and all other drugs were from Tocris Bioscience. THL was dissolved in DMSO at 10 mM, and used at 10 μM, yielding 0.1% DMSO, a concentration that does not affect striatal LTD (Gerdeman et al., 2002). All data acquisition and analysis were performed online with custom Igor Pro software. Statistical significance was evaluated using a two-tailed unpaired t-test.

Results

To determine whether psychomotor stimulation by A2A antagonists requires endocannabinoid signaling, the selective A2A antagonist SCH442416 (3 mg/kg, i.p.) was administered to three groups of mice: strain-matched wild-type controls, mice pretreated with the CB1 receptor antagonist AM251 (5 mg/kg, i.p.), and mice lacking CB1 receptors ($CB1^{-/-}$ mice) (Marsicano et al., 2002). A2A antagonist treatment significantly increased ambulatory activity in wildtype mice (Fig. 1 A, B, Table 1). Pretreatment of wildtype mice with AM251 (5 mg/kg, i.p.) had little effect on baseline ambulatory activity (105 ± 14% of wildtype baseline; $p > 0.05$; $n = 14$) but significantly attenuated the effects of SCH442416 (Fig. 1A,B, Table 1), indicating that functional CB1 receptors are required for mice to fully increase their ambulatory activity in response to an A2A antagonist. Similar results were found when we tested the effects of SCH442416 on $CB1^{-/-}$ mice. $CB1^{-/-}$ mice exhibited slightly higher baseline ambulatory activity compared with strain-matched controls of similar age (161 ± 12% of wild-type baseline; $p > 0.05$; $n = 14$). However, similar to AM251-pretreated mice, the effects of SCH442416 treatment on ambulatory activity were greatly attenuated in $CB1^{-/-}$ mice compared with wildtype vehicle-pretreated controls (Fig. 1 A, B, Table 1). SCH442416 also induced a small but significant increase in fine movements (Fig. 1C,D, Table 1). However, the increase in fine movements was not altered in AM251-treated mice or $CB1^{-/-}$ mice (Fig. 1C,D, Table 1), indicating that this feature of psychomotor activation by SCH442416 does not require endocannabinoid signaling. To verify that the increases in both ambulatory activity and fine movements that we observed were caused by SCH442416 and not by the injection procedure itself, we injected vehicle instead of SCH442416 into a subset of mice. Injection of vehicle had no effects on either type of locomotor activity (Table 1).

Our behavioral data indicate that the psychomotor effects of A2A receptor

antagonists are mediated at least in part by activation of CB1 receptors. To test whether A2A antagonists alter endocannabinoid levels in the striatum or cortex, we measured the amount of 2-AG and AEA in striatal and cortical tissue samples 5–7 min after injection of SCH442416 (3 mg/kg, i.p.) or vehicle solution. Both endocannabinoids were detectable in striatal and cortical samples from mice injected with vehicle (Fig. 2A,B). In mice injected with SCH442416, 2-AG was increased in striatum, but not cortex (Fig. 2 A). No significant differences in AEA levels were observed in striatal or cortical samples from mice injected with SCH442416 versus vehicle (Fig. 2B). Together, these results shown that A2A antagonists specifically increase the amount of striatal 2-AG.

Within the striatum, A2A receptors are highly enriched at excitatory synapses onto indirect-pathway MSNs (Rosin et al., 2003), and decreasing striatal indirect pathway function increases ambulatory activity (Durieux et al., 2009). Because the effects of SCH442416 depend on CB1 receptor activation, we tested whether it induced the release of endocannabinoids from indirect-pathway MSNs. However, application of SCH442416 (1 μM) did not alter baseline excitatory synaptic responses in indirect-pathway MSNs (supplemental Fig. 1A). We next tested whether SCH442416 could potentiate endocannabinoid-mediated LTD in indirect-pathway MSNs. First, we elicited LTD using high-frequency stimulation (100 Hz), paired with postsynaptic depolarization. Although this protocol elicited robust LTD, as previously reported (Gerdeman et al., 2002; Kreitzer and Malenka, 2007), the magnitude of LTD was not potentiated by SCH442416 (1 μM) (supplemental Fig. 1B). However, a moderate-frequency (20 Hz) stimulation protocol that elicited a small amount of LTD in control conditions gave rise to robust LTD in the presence of SCH442416 (1 μM) (88 ± 7% of baseline at 30–40 min in control conditions; 61 ± 8% of baseline at 30–40 min in SCH442416; $p < 0.05$) (Fig. 3A). Furthermore, in the presence of SCH442416, this form of LTD was blocked (102 ± 9% of

baseline at 30–40 min) (Fig. 3B) by THL (10 μM), an inhibitor of the 2-AG synthetic enzyme diacylglycerol lipase. This enhancement of 2-AG release was pathway specific, because when we delivered 20 Hz stimulation paired with postsynaptic depolarization to direct-pathway MSNs in SCH442416, no enhancement of LTD was observed (86 ± 6% of baseline at 30–40 min in control conditions; 97 ± 10% of baseline at 30–40 min in SCH442416; $p > 0.05$) (Fig. 3C). Therefore, SCH442416 selectively enhances 2-AG release and LTD induction in indirect-pathway MSNs.

Discussion

In this study, we identify a molecular mechanism underlying psychomotor activation by A2A antagonists. Specifically, we show that A2A antagonists increase striatal 2-AG and potentiate 2-AG- mediated LTD of excitatory afferents on indirect-pathway MSNs. Furthermore, blocking CB1 receptor function in vivo greatly attenuates the psychomotor stimulating effects of A2A antagonists. Our data are consistent with a model in which endocannabinoid- mediated inhibition of the indirect pathway increases movement.

These findings provide insight into a molecular mechanism for psychomotor stimulation by A2A antagonists. However, A2A receptor antagonists are certain to exhibit complex effects across numerous brain regions. In addition to the striatum, there are other potential sites of interaction between A2A receptors and endocannabinoid signaling, including the cortex and the globus pallidus. However, we do not observe any change in cortical endocannabinoid levels after A2A antagonist treatment, and in the globus pallidus, A2A transcript is not observed postsynaptically (Rosin et al., 2003), where endocannabinoids are produced. Although presynaptic interactions between A2A and CB1 receptors are possible in the globus pallidus, CB1 receptor-mediated inhibition of IPSCs is reportedly mediated by suppression of calcium influx (Engler et al., 2006), whereas A2A receptor-mediated enhancement of IPSCs is independent of calcium (Shindou et al., 2002), suggesting that these pathways act independently of each other. Furthermore, although CB1 receptors were required for the bulk of psychomotor activation by SCH442416, some psychomotor stimulation still occurred when CB1 receptor signaling was blocked (Fig. 1A,B). This remaining stimulation was likely attributable to parallel signaling pathways initiated by A2A receptor inhibition, such as decreased release of GABA in the globus pallidus (Shindou et al., 2003), which would

act synergistically with striatal 2-AG-mediated inhibition to reduce the efficacy of the indirect pathway.

We also revealed two interesting features of striatal LTD by using a moderate-frequency (20 Hz) induction protocol. First, we observed a small amount of LTD in both direct- and indirect- pathway MSNs (10–15%), consistent with the idea that endocannabinoids can be produced in both types of MSN under some experimental conditions (Narushima et al., 2006b; Shen et al., 2008b). Second, we found that indirect-pathway LTD in SCH442416 is mediated by 2-AG, whereas LTD elicited by 100 Hz stimulation is reportedly mediated by anandamide (Ade and Lovinger, 2007). Consistent with that study, we also found that striatal LTD elicited by 100 Hz stimulation is not blocked by THL (supplemental Fig. 1C). This suggests that the identity of the endocannabinoid that mediates striatal LTD can vary, depending on the experimental conditions.

A link between A2A antagonists and endocannabinoids has implications for the use of A2A antagonists to treat PD. In mouse models of PD, dopamine depletion causes a loss of endocannabinoid-dependent LTD at excitatory synapses onto indirect- pathway MSNs (Kreitzer and Malenka, 2007; Shen et al., 2008b). Our findings raise the possibility that A2A antagonists can help counter the effects of dopamine depletion by increasing endocannabinoid signaling at these synapses. Although A2A antagonists are already being investigated as PD therapeutics, our findings suggest that the efficacy of these drugs may be increased by developing compounds for human consumption that inhibit endocannabinoid degradation.

Acknowledgements

This work was supported by National Institutes of Health Grant R01 NS064984, the Pew Biomedical Scholars Program, the W. M. Keck Foundation, and the Wayne and Gladys Valley Foundation. We thank Beat Lutz for kindly providing $CB1^{-/-}$ mice; Nino Devidze, Iris Lo, Tracy Hamto, Lex Kravitz, and Philip Parker for their assistance with the behavioral experiments; and Sergi Ferré for helpful discussion.

Tables

Table 1. Psychomotor activation in mice treated with the A2A antagonist SCH442416

				Ambulatory activity		Fine movements	
Genotype	Pretreatment	Treatment	*n*	% baseline at 15–30 min	% baseline at 30 – 45 min	% baseline at 15–30 min	% baseline at 30 – 45 min
WT	Vehicle	SCH442416	13	1849 ± 363*	1038 ± 226*	160 ± 14*	136 ± 13
WT	AM251	SCH442416	14	604 ± 158*#	421 ± 136*#	183 ± 24*	172 ± 25
$CB_1^{-/-}$	Vehicle	SCH442416	14	450 ± 52*#	290 ± 45*#	157 ± 17*	118 ± 14
WT	Vehicle	Vehicle	6	94 ± 16#	69 ± 16#	96 ± 2	105 ± 4
WT	AM251	Vehicle	6	88 ± 18#	41 ± 18*#	83 ± 15	84 ± 16

Data are mean ± SEM.

*$p < 0.05$ versus baseline.

#$p < 0.05$ versus WT vehicle-pretreated SCH442416 mice.

Figures

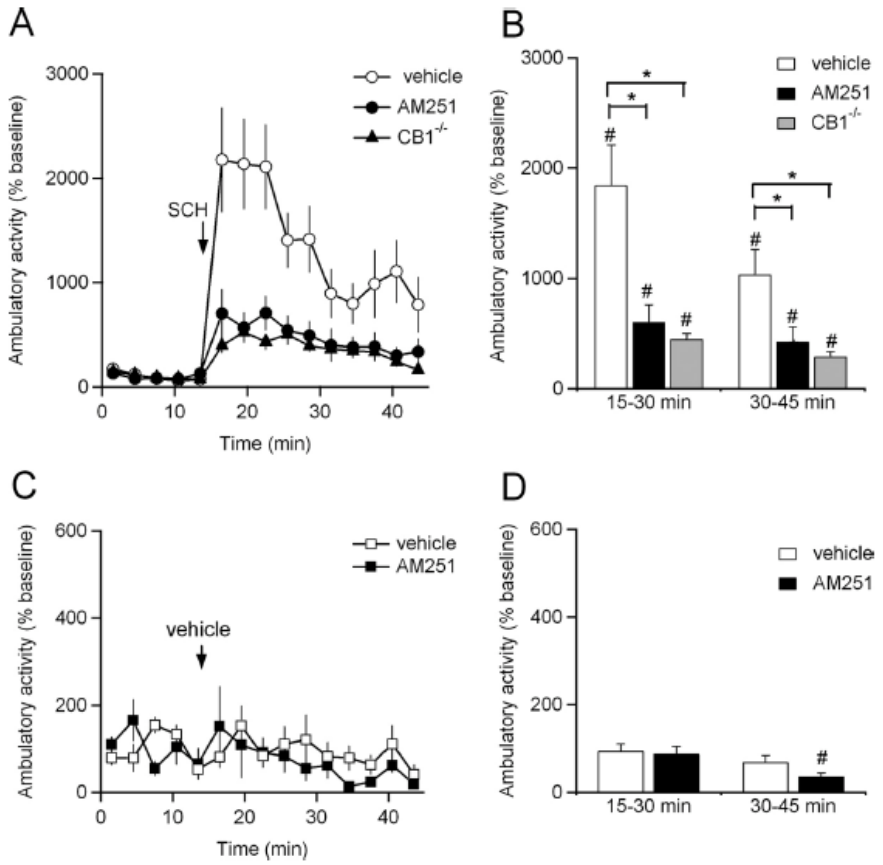

Figure 1. Stimulation of ambulatory activity by adenosine A2A antagonist treatment is attenuated by loss of cannabinoid CB1 receptor function

(A) The A2A receptor antagonist SCH442416 (3 mg/kg, i.p.) was injected into mice pretreated with vehicle (*n*=13) or the CB1 receptor antagonist AM251 (*n*=14) and into mice lacking CB1 receptors (*n*=14). Ambulatory activity is plotted.

(B) Summary of ambulatory activity at 15–30 and 30–45 min.

(C) Vehicle was injected into mice pretreated with vehicle (*n*=6) or the CB1 receptor antagonist AM251 (*n*=6). Ambulatory activity is plotted.

(D) Summary of ambulatory activity at 15–30 and 30–45 min.

In A and C, movements are binned in 3 min intervals. Pretreatment injections were given 15 min before time 0. Data are normalized to baseline activity during the first 15 min of

the experiment. *p<0.05 by one-way ANOVA with Tukey's HSD. $^{\#}p$<0.05 by two-tailed paired t-test. Data are mean ± SEM.

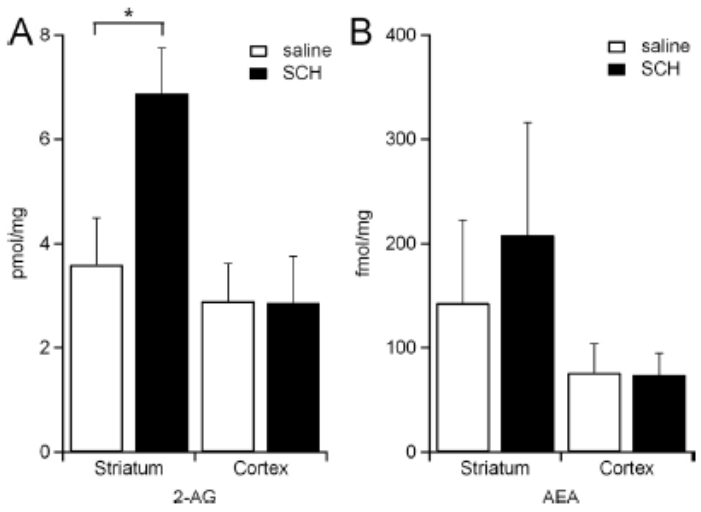

Figure 2. Adenosine A2A receptor blockade increases striatal 2-AG concentration

(A) 2-AG concentration in the striatum and cortex in mice injected with SCH442416 (3 mg/kg, i.p.) (6.9 ± 0.9 pmol/mg in striatum, *n*=6 mice; 2.8 ± 0.9 pmol/mg in cortex, *n*=6 mice) and in saline-injected controls (3.6 ± 0.9 pmol/mg in striatum, *n*=6 mice; 2.9 ± 0.7 pmol/mg in cortex, *n*=6 mice).

(B) AEA concentration in the striatum and cortex in mice injected with SCH442416 (208.1 ± 108 fmol/mg in striatum, *n*=6 mice; 73.7 ± 21 fmol/mg in cortex, *n*=3 mice) and in saline-injected controls (143.2 ± 80 fmol/mg in striatum, *n*=6 mice; 76.1 ± 28 fmol/mg in cortex, *n*=3 mice).

*p_0.05 by two-tailed unpaired *t*-test. Data are mean ± SEM.

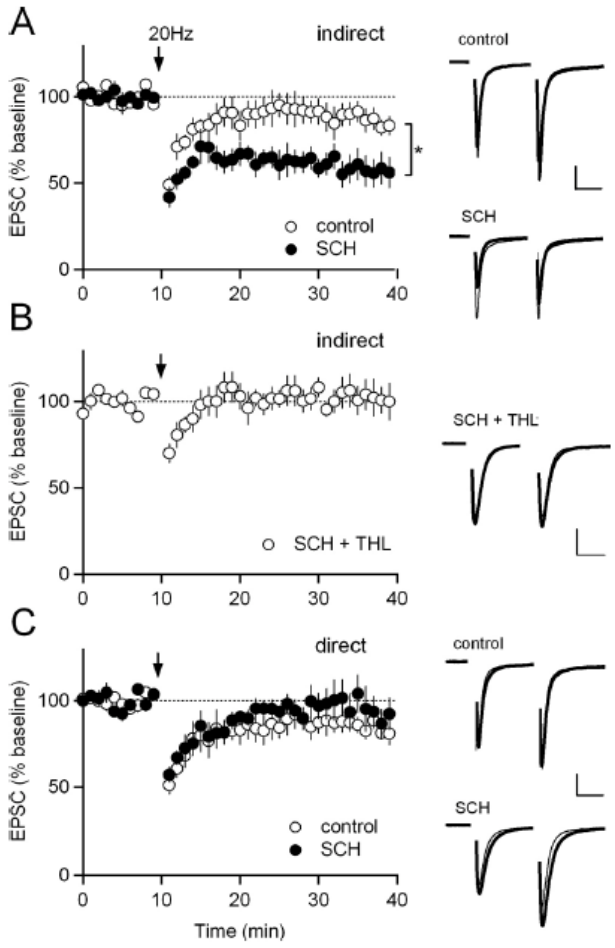

Figure 3. Adenosine A2A receptor blockade increases 2-AG-mediated synaptic depression in the indirect pathway

(A) Left, 20 Hz stimulation of afferents to indirect-pathway MSNs in control solution (*n*=6) and in 1 μM SCH442416 (SCH) (*n*=4). In this and subsequent panels, normalized EPSC amplitudes are plotted over time. The arrow indicates the time of 20 Hz stimulation, which was paired with postsynaptic depolarization to -10 mV. Right, Normalized traces from representative experiments included in A. In all example traces, the thicker gray trace is the average EPSC before 20 Hz stimulation, and the thinner black trace is the average EPSC during the last 10 min of the experiment. Calibration: 100 pA, 20 ms.

(B) Left, Twenty hertz stimulation of afferents to indirect-pathway MSNs in 1 μM

SCH442416 and 10 μM THL (*n*=6). Right, Normalized traces from representative experiments included in B.

(C) Left, Twenty hertz stimulation of afferents to direct-pathway MSNs in control solution (*n*=6) and in 1 μM SCH442416 (*n*=6). Right, Normalized traces from representative experiments included in C.

*p_0.05 by two-tailed unpaired *t* test. Data are mean ± SEM.

Supplementary Figures

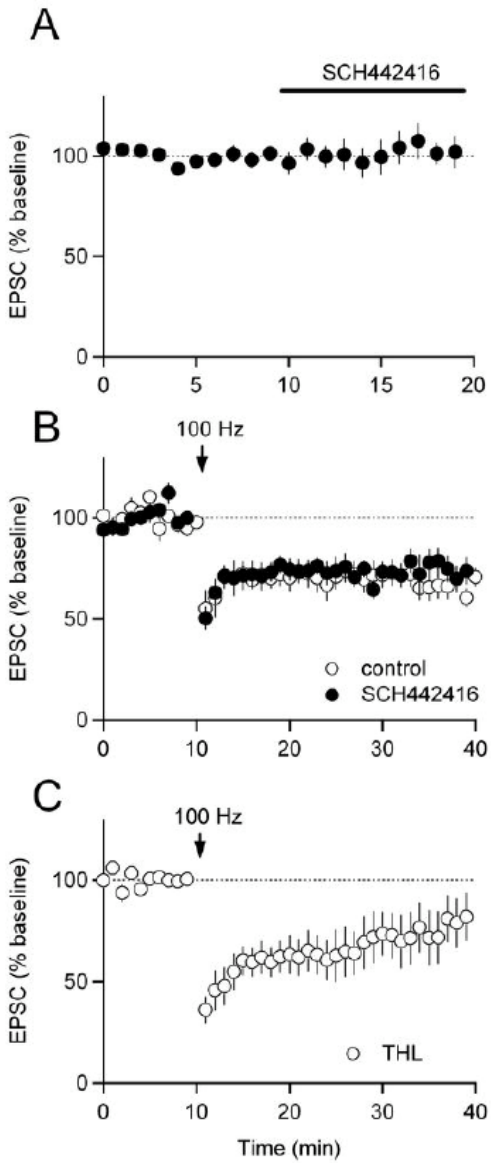

Supplementary Figure 1. Adenosine A2A receptor blockade does not depress baseline excitatory synaptic responses or high-frequency-induced LTD in indirect-pathway MSNs

(A) SCH442415 (1 μM) was washed onto the slice at the time indicated by the black bar (n=6). In this and subsequent panels, normalized EPSC amplitudes are plotted over time.

(B) 100 Hz stimulation of afferents to indirect-pathway MSNs in control solution (n=6) and in 1 μM SCH442416 (n=5). In both B and C, the arrow indicates the time of 100 Hz stimulation, which was paired with postsynaptic depolarization to -10 mV.

(C) 100 Hz stimulation of afferents to indirect-pathway MSNs in 1 μM SCH442416 and 10 μM THL (n=8).

Chapter 3

RGS4 is required for dopaminergic control of striatal LTD and susceptibility to parkinsonian motor deficits

Abstract

Plasticity of excitatory synapses onto striatal projection neurons (medium spiny neurons, or MSNs) has the potential to powerfully regulate motor function by setting the gain on signals driving both direct- and indirect-pathway basal ganglia circuits. Endocannabinoid-dependent long-term depression (eCB-LTD) is the best characterized form of striatal plasticity, but the mechanisms governing its normal regulation and pathological dysregulation are not well understood. We characterized two distinct biochemical signaling pathways mediating eCB production in striatal indirect-pathway MSNs: a PLCβ- and DAG lipase-dependent pathway that is engaged by low-frequency stimulation, and a novel Src- and PLD-dependent pathway that is engaged by high-frequency stimulation. Endocannabinoid production through both pathways was modulated by dopamine D2 and adenosine A2A receptors, acting through cAMP/PKA. We identified Regulator of G-protein Signaling 4 (RGS4) as a key link between D2/A2A signaling and eCB mobilization pathways. In contrast to wildtype mice, $RGS4^{-/-}$ mice exhibited normal eCB-LTD in the presence of A2A agonists, or D2 receptor antagonists, or after dopamine depletion. Furthermore, $RGS4^{-/-}$ mice were significantly less impaired in the 6-OHDA model of Parkinson's disease. Taken together, these results support a model in which dysregulation of eCB-LTD through D2/A2A signaling is critical for the

emergence of parkinsonian motor deficits, and suggest that inhibition of RGS4 may represent an effective non-dopaminergic strategy for treating Parkinson's disease.

Introduction

The basal ganglia are a network of subcortical brain nuclei engaged in many aspects of motor function, including action selection, motor skill acquisition, and habit formation (Graybiel et al., 1994; Hikosaka et al., 2000; Packard and Knowlton, 2002; Yin and Knowlton, 2006). Information enters the basal ganglia through the striatum, whose principal neurons (medium spiny neurons, or MSNs) receive highly convergent excitatory input from the cortex and thalamus (Bolam et al., 2000). The excitatory synapses formed onto MSNs are an important site of long-term plasticity in the basal ganglia network (Kreitzer and Malenka, 2008; Lerner and Kreitzer, 2011; Surmeier et al., 2009). This plasticity has the potential to powerfully regulate basal ganglia circuit function, and therefore motor function, by setting the gain on incoming cortical and thalamic signals. Defects in striatal plasticity are thought to play a role in many movement disorders including Parkinson's disease, Huntington's disease, and dystonia (Kitada et al., 2009; Kitada et al., 2007; Kreitzer and Malenka, 2007; Kurz et al., 2010; Peterson et al., 2010; Shen et al., 2008b).

Despite its functional importance, the molecular mechanisms underlying striatal plasticity remain elusive. The best-studied form of striatal plasticity is endocannabinoid-dependent LTD (eCB-LTD). This form of LTD is induced following the production and release of endocannabinoids (eCBs) from the postsynaptic neuron, which then act on presynaptic CB1 receptors to lower neurotransmitter release probability. Although eCB-LTD is observed in both subtypes of MSNs (Shen et al., 2008b), it can be most reliably induced *in vitro* at excitatory synapses onto indirect-pathway MSNs (Kreitzer and Malenka, 2007), which express dopamine D2 and adenosine A2A receptors. There are several postsynaptic membrane proteins that are required to elicit eCB release sufficient to induce indirect-pathway eCB-LTD: group I (G_q-coupled) metabotropic glutamate

receptors (mGluRs), L-type voltage-gated calcium channels (L-VGCCs), and dopamine D2 receptors (Calabresi et al., 1994; Calabresi et al., 1997; Choi and Lovinger, 1997; Kreitzer and Malenka, 2005; Sung et al., 2001). Adenosine A2A receptors are also able to modulate indirect-pathway LTD (Lerner et al., 2010; Shen et al., 2008b). Previous work has established the importance of postsynaptic activation of group I mGluRs and L-VGCCs (Calabresi et al., 1994; Choi and Lovinger, 1997; Sung et al., 2001), yet it is not known how the signaling pathways of these two membrane proteins interact. It has also been proposed that phospholipase Cβ (PLCβ) is a coincidence detector for group I mGluR activation of G_q signaling and calcium influx through L-VGCCs (Fino et al., 2010; Hashimotodani et al., 2005). However, the precise role of PLCβ in striatal eCB-LTD is not clear (Adermark and Lovinger, 2007).

Similarly, it remains unclear why activation of D2 receptors is required for eCB-LTD, or why blockade of A2A receptors enhances it. One study indicated that D2 receptors act via adenylyl cyclase 5 (Kheirbek et al., 2009), but what occurs downstream of cAMP production is not known. Other studies have questioned whether the D2 receptors that modulate LTD are located on MSNs or on cholinergic interneurons (Tozzi et al., 2011; Wang et al., 2006). Understanding how dopamine receptors control striatal function is especially important in the context of Parkinson's disease, where dopaminergic input to the striatum is lost. For many decades, Parkinson's patients have been treated with the dopamine precursor levodopa and more recently with dopamine receptor agonists (typically D2-receptor-specific agonists). While this direct approach of dopamine replacement is extremely helpful in relieving symptoms early in the disease process, as the disease progresses its efficacy wanes and side effects often develop. A better understanding of how dopamine acts in the striatum could lead to new strategies for treating Parkinson's disease symptoms downstream of dopamine receptors.

Ultimately, the signaling pathways of group I mGluRs, L-VGCCs, D2 receptors and A2A receptors must converge to control the postsynaptic mobilization of eCBs. However, the specific pathways underlying eCB mobilization for striatal LTD—and the putative eCB produced—are not clear. There are two major candidates: (1) anandamide (AEA), thought to be produced by phospholipase D (PLD) activity, and (2) 2-arachidonoylglycerol (2-AG), thought to be produced by PLCβ and DAG lipase (Ahn et al., 2008; Piomelli, 2003). Much of the available evidence has supported the role of AEA in indirect-pathway LTD (Ade and Lovinger, 2007; Giuffrida et al., 1999; Kreitzer and Malenka, 2007). However, 2-AG can also mediate LTD (Fino et al., 2010; Lerner et al., 2010). Additionally, 2-AG appears to be the major signaling endocannabinoid for plasticity in other brain areas as well as for short-term endocannabinoid-dependent plasticity in the striatum (Gao et al., 2010; Tanimura et al., 2010; Uchigashima et al., 2007).

In this study, we outline a model of striatal eCB production that clarifies the role of group I mGluRs, internal calcium stores, and L-VGCCs during LTD induction by both low- and high-frequency stimulation protocols. We also provide a mechanism for the control of eCB production by D2 and A2A receptors in striatal MSNs. Specifically, we find that a GTPase-activating protein called Regulator of G-protein Signaling 4 (RGS4) links D2 and A2A signaling to group I mGluR signaling. These findings unify a number of previously disparate findings related to striatal eCB-LTD, and raise the possibility of new non-dopaminergic drugs to treat Parkinson's disease.

Material and Methods

Electrophysiology. Coronal brain slices (300 μm thick) containing the striatum were prepared from Drd2-GFP heterozygous (+/-) BAC transgenic mice on the C57BL/6 background (postnatal days 21–35) unless otherwise stated. Other mouse lines used for electrophysiology were RGS4-/- Drd2-GFP +/- mice on the C57BL/6 background and Drd1-tomato+/- mice on the FVB background. The Institutional Animal Care and Use Committee of the University of California, San Francisco approved all experiments. Slices were superfused with an external solution containing the following (in mM): 125 NaCl, 2.5 KCl, 2 CaCl2, 1 MgCl2, 26 NaHCO3, 1.25 NaH2PO4-H2O, and 12.5 glucose, bubbled with 95% O2/5% CO2. When drugs were added to the external solution, they were first dissolved in water or DMSO, then diluted into the external solution. The final concentration of DMSO in the external solution was always ≤0.1%, a concentration that does not affect striatal LTD (Gerdeman et al., 2002). Slices were allowed to recover for at least 1 h before recording. Whole-cell voltage-clamp recordings from indirect-pathway MSNs were obtained from visually identified GFP-positive MSNs in dorsolateral striatum in Drd2-GFP mice or from tomato-negative MSNs in the dorsolateral striatum in Drd1-tomato mice where noted. All recordings were performed at a temperature of 30-32°C, with picrotoxin (50 μM) present to suppress $GABA_A$-mediated currents. Resistance of the patch pipettes was 2.5–4MΩ when filled with intracellular solution containing the following (in mM): 120 CsMeSO3,15 CsCl, 8 NaCl, 0.2 EGTA, 10 HEPES, 2 Mg-ATP, 0.3 Na-GTP, 10 TEA (tetraethylammonium), 5 QX-314 (lidocaine *N*-ethyl bromide), adjusted to pH 7.25 with CsOH. When drugs were added to the intracellular solution, they were first dissolved in water or DMSO at 1000x and then diluted into the intracellular solution. When a drug had been added to the intracellular solution, LTD was

not induced for at least 15 min after break-in to ensure that the drug had time to diffuse into the neuronal processes. MSNs were held at -70 mV, and excitatory synaptic currents (EPSCs) were evoked by intrastriatal microstimulation with a saline-filled glass pipette placed 50 –100 μm dorsolateral of the recorded neuron. Stimulation intensity was adjusted to yield 300-500 pA EPSCs. Test pulses, which consisted of two stimuli 50 ms apart, were given every 20 s. To evoke LTD, MSNs were stimulated at 20 or 100 Hz for 1 s, paired with postsynaptic depolarization to -10 mV. For HFS-LTD, 100 Hz stimulation was repeated 4 times at 10 s intervals. For LFS-LTD, 20 Hz stimulation was repeated 30 times at 10 s intervals. During LTD, stimulation intensity was increased 2.5 fold to ensure robust induction. All data acquisition and analysis was performed online with custom Igor Pro software. Statistical significance was evaluated using two-tailed unpaired t tests. All drugs were purchased from Tocris Bioscience, except ddATP (catalog # D0939 from Sigma), CAY10594 and CAY10593 (from Cayman Chemical), Sp-8-OH-cAMPS (from Biolog), and CCG-63802 (from Chem Div). RGS4 recombinant protein was purchased from Genway.

6-OHDA injections. Mice were unilaterally injected with 6-OHDA at 3 weeks of age (for recordings) or 7 weeks of age (for behavior). Ten minutes before surgery, mice were given desipramine (25 mg/kg i.p., Sigma) to block norephinephrine transporters. Anesthesia was induced with a mixture of ketamine and xylazine (80 mg ketamine plus 20 mg xylazine per kg of body weight, i.p.) and maintained with isoflurane through a nose cone mounted on a stereotaxic apparatus (Kopf Instruments). Scalp hair was removed using Nair and the skin was cleaned with a povidone-iodine antiseptic. The scalp was opened and a hole was drilled in the skull (-0.6 mm AP, ±1.2mm ML from bregma for 3 week old mice, -1.0 mm AP, ±1.2mm ML from bregma for 7 week old mice). 6-OHDA (1μl, 5 mg/mL for recordings, 2 mg/mL for behavior) was injected into the

medial forebrain bundle (−5.0 mm DV from top of brain) through a 33-gauge steel injector cannula (PlasticsOne) using a syringe pump (World Precision Instruments) that infused the 6-OHDA over 5 min. The injection cannula was left in place for 5 min following the injection and then slowly removed. After surgery, mice were given buprenorphine (0.1 mg/kg, i.p.) and ketoprofen (5 mg/kg, s.c.) as analgesics and allowed to recover on a heated pad.

Open Field Behavior. Mice were placed in a round (10" diameter) activity chamber for 10 minutes (for unilateral 6-OHDA injection experiments) or a square (15" x 15") activity chamber for 30 minutes (for bilateral 6-OHDA injection experiments) and video-monitored from above. Testing was performed in a dimly lit room. The activity chambers were cleaned with 70% ethanol between sessions. The positions of the nose, tail and center of mass of each mouse were tracked using ETHOVISION 7 software (Noldus). A smoothing algorithm was applied to all video tracks before analysis to reduce system noise (locally weighted scatterplot smoothing based on ten points before and after each data point, performed in ETHOVISION 7). Ambulation was defined as movement of the center of mass greater than 2 cm/s. Fine Movement was defined as movement of the center of mass less than 1.75 cm/s with greater than 2% of pixels in the image changing. Freezing was defined as movement of the center of mass of less than 1.75 cm/s with less than 2% of pixels in the image changing. Rotations were defined as full 360º turns during which the mouse turned back in the other direction <90º before completing the turn. Statistical significance was evaluated using a two-way ANOVA with Tukey's honestly significant difference.

Balance Beam Behavior. Mice were trained to walk across a 35 cm Plexiglas beam (Tap Plastics) elevated 50 cm above the floor to reach a dark, enclosed box. Training

consisted of two guided trials and six unguided trials on a round 1 cm diameter beam the day before testing. Testing consisted of three unguided trials on a rectangular 0.5 cm thick beam. Training and testing were performed in a well-lit room. The beams were cleaned with 70% ethanol between training and testing sessions of each mouse. Slips on and falls off the balance beam were recorded for later analysis. Statistical significance was evaluated using a two-way ANOVA with Tukey's honestly significant difference.

Tyrosine Hydroxylase (TH) staining. To confirm dopamine depletion in acute slices (300 μm thick) used for recording, the slices were fixed in 4% paraformaldehyde (PFA) overnight at 4 ºC and then equilibrated in 30% sucrose in PBS before resectioning. To produce 30 μm sections for immunostaining, the 300 μm slices were resectioned on a SM2010R freezing microtome (Leica) and stored in PBS until staining. To confirm dopamine depletion in mice used for behavior, mice were perfused with 4% PFA in the afternoon after their behavioral data were collected. Their brains were left to fix in 4% PFA overnight at 4 ºC and then equilibrated in 30% sucrose in PBS before sectioning. Sections (30 μm) were made on a SM2010R freezing microtome (Leica) and stored in PBS until staining. After 30 μm sections were created from 300 μm slices or whole brains, all tissue was stained using the same protocol. Tissue was blocked with 10% normal donkey serum and permeabilized with 0.1% Triton-X-100. Primary antibody incubation was performed at 4ºC for 24 hr, using rabbit anti-TH (1:200, Pel-Freeze). Secondary antibody, goat anti-rabbit (1:500, Vector Labs) was incubated for 1 hour at room temperature. Images were taken on a 6D epifuorescent microscope (Nikon) and quantified using ImageJ software. For unilateral 6-OHDA injections, the intensity of fluorescence on the ipsilateral side was compared to that on the contralateral side for each mouse with the intensity of fluorescence in an image of the septum subtracted as

background. Only mice with ≤5% residual TH staining on the ipsilateral side were included in the analysis. For bilateral 6-OHDA injections, the average intensity of fluorescence in the two striata of each 6-OHDA-injected mouse was compared to the average intensity of fluorescence in the two striata of an uninjected control mouse of the same genotype with the intensity of fluorescence in an image of the septum subtracted as background. Only mice with comparable, ≤35% residual TH staining in both dorsolateral striata were included in the analysis.

Results

PLCβ-dependent and -independent forms of eCB-LTD can be elicited at excitatory synapses onto striatal indirect-pathway MSNs

To study the mechanisms of eCB-LTD in indirect-pathway MSNs, we began by confirming that high-frequency stimulation (HFS; 100 Hz) of excitatory afferents to indirect-pathway MSNs in the dorsolateral striatum causes eCB-LTD when paired with postsynaptic depolarization (48 ± 2% of baseline at 30-40 min in control conditions; 97 ± 6% of baseline at 30-40 min in the cannabinoid CB1 receptor antagonist AM251; $p<0.05$; Fig. 1A-B). We also confirmed that HFS-LTD is dependent on group I (G_q-coupled) mGluRs by bath application of the group I mGluR antagonist AIDA (96 ± 12% of baseline at 30-40 min, $p<0.05$ compared to control; Fig.1C). Next, we tested potential signaling pathways downstream of G_q. The canonical target of G_q is PLCβ (Hubbard and Hepler, 2006; Taylor et al., 1991). Surprisingly, we were unable to block HFS-LTD by including the PLC inhibitor U73122 in the intracellular recording solution (54 ± 5% of baseline at 30-40 min; Fig. 1C). This finding was unexpected because other groups have demonstrated that endocannabinoid-mediated depression in MSNs is PLCβ-dependent (Fino et al., 2010; Hashimotodani et al., 2005; Jung et al., 2005; Yin and Lovinger, 2006), although not in all cases (Adermark and Lovinger, 2007). Therefore, we decided to examine whether the PLCβ-independence of HFS-LTD was peculiar to that stimulation protocol.

As an alternative to HFS-LTD, we applied a low-frequency stimulation (LFS) induction protocol that is qualitatively similar to that used in previous studies of striatal LFS-LTD (Lerner et al., 2010; Ronesi and Lovinger, 2005). In brief, we repeatedly paired

epochs of 20 Hz stimulation with postsynaptic depolarization over several minutes (see methods for details) to induce LTD (56 ± 10% of baseline at 30-40 min; Fig. 1D, E). Similar to HFS-LTD, LFS-LTD was blocked by AM251 and AIDA (95 ± 6% of baseline at 30-40 min in AM251; 100 ± 8% of baseline at 30-40 min in AIDA; both $p<0.05$ compared to control; Fig. 1E-F), indicating a dependence on CB1 receptors and group I mGluRs, respectively. However, LFS-LTD was also blocked by intracellular U73122 (102 ± 15% of baseline at 30-40 min; $p<0.05$ compared to control; Fig. 1F), indicating a role for PLCβ. Thus, both PLCβ-dependent and -independent forms of eCB-LTD can be elicited at excitatory synapses onto striatal indirect-pathway MSNs simply by using different stimulation frequencies and repetitions.

LFS-LTD requires DAG lipase, but not elevations in intracellular calcium

PLCβ is an enzyme that produces the intracellular secondary messenger diacylglycerol (DAG), which can be converted to the endocannabinoid 2-arachidonylglycerol (2-AG) by the enzyme DAG lipase (DAGL). The sequential activities of PLCβ and DAGL represent a well-defined pathway for 2-AG production that could mediate LFS-LTD. To test whether DAGL is also required for LFS-LTD, we applied the LFS-LTD induction protocol in the presence of the DAGL inhibitor THL and observed that THL blocked LFS-LTD (92 ± 13% of baseline at 30-40 min; $p<0.05$ compared to control; Fig. 2A).

In addition to DAG, PLCβ produces another important secondary messenger, IP_3, which can activate IP_3 receptors located on the endoplasmic reticulum and cause release of calcium from internal stores. To test whether internal calcium stores are involved in LFS-LTD, we added thapsigargin, which depletes these stores, to our

intracellular recording solution, but this manipulation did not block LFS-LTD (47 ± 7% of baseline at 30-40 min; Fig. 2B).

Although internal calcium stores were not required for LFS-LTD, other sources of calcium might be important. L-type voltage-gated calcium channels (L-VGCCs) have previously been implicated in eCB release (Adermark and Lovinger, 2007; Calabresi et al., 1994; Choi and Lovinger, 1997; Kreitzer and Malenka, 2005), yet we found that the L-VGCC blocker nitrendipine did not block LFS-LTD (64 ± 6% of baseline at 30-40 min; Fig. 2C). Another L-VGCC blocker, nifedipine, also did not block LFS-LTD (64 ± 10% of baseline at 30-40 min, n=6, data not shown). In fact, elevations in intracellular calcium do not appear to be strictly required for LFS-LTD, since loading MSNs with the calcium-chelator BAPTA did not block LFS-LTD (75 ± 10% of baseline at 30-40 min; Fig. 2C). From these experiments, we conclude that the most likely scenario for LFS-LTD induction is that activation of G_q-coupled mGluRs leads to activation of PLCβ, stimulating the production of DAG, which is then converted to 2-AG by DAGL (Fig. 2D).

HFS-LTD requires elevations in intracellular calcium mediated by L-type calcium channels and calcium-induced calcium release

Our initial experiments (Fig. 1) showed that the pathways underlying HFS-LTD and LFS-LTD diverge after just one step in their induction pathways (activation of G_q by group I mGluRs). Because HFS-LTD is PLCβ-independent (Fig. 1C), we predicted it would be DAGL-independent as well. Indeed, as observed previously (Ade and Lovinger, 2007; Lerner et al., 2010), the DAGL inhibitor THL did not block HFS-LTD (61 ± 10% of baseline at 30-40 min; Fig. 3A). We also tested whether HFS-LTD differed from LFS-LTD in its requirements for calcium. By adding thapsigargin to our intracellular

solution to deplete internal calcium stores, we found that, unlike LFS-LTD, HFS-LTD requires these stores (117 ± 17% of baseline at 30-40 min; $p<0.05$ compared to control; Fig. 3B). Calcium from internal stores can be released into the cytoplasm via either IP_3 receptors or ryanodine receptors (RyRs). Since HFS-LTD does not require PLCβ, which produces IP_3, we reasoned that the requirement for internal calcium stores in HFS-LTD was more likely to be dependent on RyRs than IP_3 receptors. Indeed, when RyRs were inhibited by including ryanodine in the intracellular solution, HFS-LTD was blocked (108 ± 8% of baseline at 30-40 min; $p<0.05$ compared to control) (Fig. 3B). An IP_3 receptor blocker, 2-APB, did not block HFS-LTD when included in the intracellular solution (63 ± 10% of baseline at 30-40 min; Supp. Fig. 2A).

RyRs are activated by calcium and, once activated, cause the release of more calcium into the cytoplasm. This process of calcium-induced calcium release (CICR) serves to amplify calcium signals initiated by other sources of calcium influx. What is the CICR-initiating source of calcium in HFS-LTD? We consider L-VGCCs to be a likely source, because they are functionally coupled to RyRs (Chavis et al., 1996) and because L-VGCCs have previously been shown to be involved in striatal LTD (Calabresi et al., 1994; Choi and Lovinger, 1997). In agreement with this hypothesis, the L-VGCC antagonist nitrendipine blocked HFS-LTD (92 ± 4% of baseline at 30-40 min; $p<0.05$ compared to control; Fig. 3C).

HFS-LTD requires Src kinase and phospholipase D

Why does HFS-LTD require group I mGluRs if it is PLCβ-independent? We reasoned that G_q must activate another enzyme in addition to PLCβ. Other direct targets of G_q include non-receptor tyrosine kinases (Bence et al., 1997). Src-family kinases are

non-receptor tyrosine kinases that phosphorylate a number of targets linked to endocannabinoid mobilization, including L-type calcium channels and phospholipase D (PLD) (Bence-Hanulec et al., 2000; Henkels et al., 2010). Therefore, to test whether Src-family kinases are required for HFS-LTD, we attempted to induce HFS-LTD in the presence of the Src-family kinase inhibitor PP2. PP2 completely blocked HFS-LTD (105 ± 16% of baseline at 30-40 min; $p<0.05$ compared to control; Fig.3D). To further test the hypothesis that postsynaptic Src, specifically, is required for HFS-LTD, we next included a membrane impermeable c-Src inhibitor peptide in our intracellular recording solution. This inhibitor peptide was also able to block HFS-LTD (88 ± 5% of baseline at 30-40 min; $p<0.05$ compared to control; Fig. 3D). Notably, the Src inhibitor PP2 did not block LFS-LTD (62 ± 3% of baseline at 30-40 min; Supp. Fig. 1A), indicating that Src acts specifically in HFS-LTD induction.

We next explored whether Src activation and the rise in intracellular calcium due to L-VGCCs and CICR could be connected to any of the known or posited PLCβ-independent eCB production pathways. Since we had already observed that inhibiting the major 2-AG production enzyme DAGL did not block HFS-LTD (Fig. 3A), we explored a possible role for enzymes proposed to mediate anandamide (AEA) biosynthesis. AEA can be produced by a number of different synthesis pathways. Key enzymes in these various pathways include PLC, PLA_2, and PLD (PLD1, PLD2, or NAPE-specific PLD) (Ahn et al., 2008). A role for any PLC isoforms had already been ruled out by our experiments with the general PLC inhibitor U73122 (Fig. 1C). A PLA_2 inhibitor, OBAA, also did not prevent HFS-LTD (57 ± 1% of baseline at 30-40 min; Supp. Fig. 2B). Finally, mice lacking NAPE-specific PLD have intact AEA levels (Leung et al., 2006), arguing against an essential role of that PLD isoform. However, an inhibitor of PLD (with some specificity for PLD2 over PLD1), CAY10594, significantly blocked HFS-LTD (82 ± 5% of

baseline at 30-40 min; $p<0.05$ compared to control; Fig. 3E). Another PLD inhibitor, CAY10593, also blocked HFS-LTD to a similar degree (85 ± 10% of baseline at 30-40 min, n=3, data not shown). We conclude that PLD is a key enzyme for eCB mobilization in response to HFS. These data lead us to propose a model for HFS-LTD in which activation of G_q-coupled mGluRs leads to activation of Src, stimulating the production of AEA by PLD, either by modulating PLD function directly (Henkels et al., 2010) or by modulating L-VGCCs (Bence-Hanulec et al., 2000) (Fig. 3F).

Dopamine D2 and adenosine A2A receptors modulate both LFS- and HFS-LTD

Because HFS-LTD and LFS-LTD are mediated by distinct signaling pathways downstream of G_q, we wondered whether they are both modulated by dopamine D2 or adenosine A2A receptors. It is established that HFS-LTD in indirect-pathway MSNs requires dopamine D2 receptors (Kreitzer and Malenka, 2007; Shen et al., 2008b). However, D2 receptor activation alone is not sufficient to induce endocannabinoid signaling; coincident group I mGluR activation is required (Supp. Fig. 3). We confirmed that the D2 receptor antagonist sulpiride blocked HFS-LTD (103 ± 8% of baseline at 30-40 min; $p<0.05$ compared to control; Fig. 4A). Interestingly, sulpiride was also able to inhibit LFS-LTD (88 ± 4% of baseline at 30-40 min; $p<0.05$ compared to control; Fig. 4B), indicating that D2 receptors act on eCB-LTD at or upstream of G_q.

Adenosine A2A receptors are also highly expressed in indirect-pathway MSNs, where they influence endocannabinoid signaling and act in opposition to D2 receptors (Shen et al., 2008b; Tozzi et al., 2007). Therefore, we tested whether activation of A2A receptors could block HFS- or LFS-LTD. The A2A receptor agonist CGS21680 blocked both HFS- and LFS-LTD (102 ± 7% of baseline at 30-40 min; $p<0.05$ compared to

control for HFS-LTD; 90 ± 12% of baseline at 30-40 min; $p<0.05$ compared to control for LFS-LTD; Fig. 4C, D). Thus, like D2 receptors, A2A receptors appear to be acting at or upstream of G_q to modulate both forms of eCB-LTD in indirect-pathway MSNs. We confirmed these results in two different BAC transgenic mouse strains (Drd2-EGFP, target EGFP-positive MSNs; Drd1a-Tmt, target Tmt-negative MSNs), indicating that D2/A2A regulation is robust across multiple mouse lines (Supp. Fig. 2C).

Dopamine D2 and adenosine A2A receptors modulate eCB-LTD through cAMP/PKA signaling

We next considered how D2 and A2A receptors modulate eCB mobilization and LTD. Because regulation of eCB biosynthetic pathways by cAMP/PKA signaling is not well established, we first tested whether D2 receptors act to promote eCB-LTD through a reduction in cAMP levels or PKA activation. In this and subsequent experiments, we utilized HFS-LTD to examine the mechanisms regulating eCB-LTD, because this form of LTD remains a standard in the field. To examine whether inhibition of cAMP production alone is sufficient to enable eCB-LTD induction, even in the presence of a D2 receptor antagonist, we used a membrane-impermeable adenylyl cyclase inhibitor, ddATP, and a membrane-impermeable inhibitor of PKA, PKI, which were added to our intracellular recording solution. The membrane-impermeability of these drugs limited their effects to the recorded postsynaptic MSN, which allowed us to rule out effects on cAMP/PKA-dependent processes in the presynaptic terminal or in neighboring MSNs or interneurons. With either ddATP or PKI in our intracellular recording solution, we were able to elicit LTD in the presence of sulpiride (69 ± 9% of baseline at 30-40 min with

sulpiride and ddATP; 71 ± 10% of baseline at 30-40 min with sulpiride and PKI; both $p<0.05$ compared to LTD in sulpiride alone; Fig. 5A).

In contrast to the action of D2 receptors, A2A receptors are G_s-coupled receptors, and we therefore hypothesized that activation of A2A receptors blocks LTD by increasing cAMP/PKA signaling. In support of this hypothesis, we found that reducing cAMP/PKA activity by including either ddATP or PKI in the intracellular recording solution allowed LTD to occur in the presence of A2A agonist CGS21680 (61 ± 4% of baseline at 30-40 min with CGS21680 and ddATP; 65 ± 7% of baseline at 30-40 min with CGS21680 and PKI; both $p<0.05$ compared to LTD in CGS21680 alone; Fig. 5B). To verify that the LTD that occurs when cAMP/PKA signaling is inhibited is actually eCB-LTD and not another form of synaptic plasticity, we added the CB1 receptor antagonist AM251 to an extracellular recording solution which already contained CGS21680 and patched cells with PKI included in the intracellular solution. The addition of AM251 to the extracellular solution blocked LTD (119 ± 16% of baseline at 30-40 min; $p<0.05$ compared to LTD with CGS21680 and PKI; Supp. Fig. 2D), demonstrating that cAMP/PKA inhibition is allowing eCB-LTD to occur.

To further test the hypothesis that increases in cAMP/PKA signaling are sufficient to block LTD, we tested whether directly activating either adenylyl cyclase or PKA would block HFS-LTD when there were no drugs present in the external saline solution. To activate adenylyl cyclase we used the water-soluble (membrane-impermeable) forskolin analog NKH477. To activate PKA we used a membrane-impermeable PKA activator, Sp-8-OH-cAMPS. When either NKH477 or Sp-8-OH-cAMPS were included in our intracellular recording solution, LTD was inhibited (78 ± 5% of baseline at 30-40 min with NKH477; 89 ± 9% of baseline at 30-40 min with Sp-8-OH-cAMPS; both $p<0.05$

compared to control LTD; Fig. 5C, D). From these experiments, we concluded that increased cAMP/PKA activity inhibits LTD.

D2 and A2A receptors regulate striatal LTD via Regulator of G-protein Signaling 4 (RGS4)

How does cAMP/PKA activity block LTD? Because D2 and A2A receptor drugs act on both LFS- and HFS-LTD, they likely act on a common target in both pathways: group I mGluRs or G_q. A particularly attractive candidate for such modulation is Regulator of G protein signaling 4 (RGS4). RGS4 is a GTPase-activating protein expressed strongly in MSNs in the dorsolateral striatum, where it is associated with mGluR5 and PLCβ (Gold et al., 1997; Schwendt and McGinty, 2007), its activity is increased by PKA phosphorylation (Huang et al., 2007), and it strongly inhibits signaling through G_q (Saugstad et al., 1998).

To test whether RGS4 is involved in the regulation of LTD by D2 and A2A receptors, we obtained RGS4$^{-/-}$ mice, crossed those mice into our D2-EGFP BAC transgenic line so that we could identify indirect-pathway MSNs, and applied the HFS-LTD induction protocol to indirect-pathway MSNs. In RGS4$^{-/-}$ mice, we observed significant HFS-LTD (66 ± 5% of baseline at 30-40 min; Fig. 6A). If RGS4 is responsible for the connection between D2 and A2A receptor signaling and G_q signaling, then LTD in RGS4$^{-/-}$ mice should occur even in the presence of the D2 antagonist sulpiride or the A2A agonist CGS21680. Indeed, LTD was readily observed in the presence of either drug in RGS4$^{-/-}$ mice (80 ± 6% of baseline at 30-40 min in sulpiride; 64 ± 7% of baseline at 30-40 min in CGS21680; Fig. 6B).

While genetic knockouts offer complete elimination of the gene product, they also may yield developmental and/or homeostatic changes. Therefore, we used a recently identified small-molecule inhibitor of RGS4, CCG-63802 (Blazer et al., 2010), to test whether acute inhibition of RGS4 could uncouple LTD from D2 receptors. CCG-63802 was included in the intracellular recording solution to restrict the drug to the postsynaptic neuron, which also allowed us to ask whether RGS4 was acting cell autonomously. With CCG-63802 in the pipette, the magnitude of LTD in control solution and in the presence of sulpiride was indistinguishable (76 ± 10% of baseline at 30-40 min with CCG-63802; 70 ± 12% of baseline at 30-40 min with CCG-63802 in sulpiride; Fig. 6C). Thus, we conclude that RGS4 is acting acutely in the postsynaptic neuron to modulate LTD.

We also tested whether replacing RGS4 protein in indirect-pathway MSNs from $RGS4^{-/-}$ mice could rescue the modulation of LTD by D2 and A2A receptors. We loaded different concentrations of recombinant RGS4 protein into the pipette and obtained whole-cell recordings from indirect-pathway MSNs in $RGS4^{-/-}$ mice. We found that the effects of loading recombinant RGS4 into the MSN were highly dose-dependent (Supp. Fig. 4). A low concentration (10 pM) of RGS4 allowed LTD to occur but did not restore the modulation of LTD by D2 and A2A receptors seen in wildtype mice. A higher concentration (50 pM) of RGS4, completely blocked LTD, presumably because G_q signaling was constitutively inhibited by an excess of RGS4. However, an intermediate concentration (25 pM) of RGS4 did not block LTD on its own but enabled LTD to be blocked by either sulpiride or CGS21680 (66 ± 6% of baseline at 30-40 min with 25 pM RGS4; 84 ± 2% of baseline at 30-40 min with 25 pM RGS4 in sulpiride; 96 ± 5% of baseline at 30-40 min with 25 pM RGS4 in CGS21680; LTD with 25 pM RGS4 was significantly different from LTD with 25 pM RGS4 in either sulpiride or CGS21680, $p<0.05$; Fig. 6D). This result demonstrates that there is a concentration of RGS4 protein

that allows for fast, dynamic regulation of its activity, likely via PKA phosphorylation (Huang et al., 2007). The fact that replacement of RGS4 protein only in the postsynaptic MSN was able to rescue D2 and A2A receptor modulation of LTD in RGS4$^{-/-}$ mice argues against developmental defects contributing to the changes in LTD in the knockout mice, and provides further support for a cell-autonomous action of RGS4.

Indirect-pathway LTD in RGS4$^{-/-}$ mice is resistant to dopamine depletion

The striatum receives dense dopaminergic innervation from the substantia nigra pars compacta, and dopamine is required for proper striatal function. When dopaminergic innervation of the striatum is lost, as occurs in humans with Parkinson's disease, motor function is severely impaired. Similarly, when striatal dopamine is depleted in mice by injecting the toxin 6-OHDA into the medial forebrain bundle (where dopaminergic axons exit the substantia nigra pars compacta), parkinsonian motor behaviors, such as increased immobility and decreased ambulation are observed. At least part of the inhibition of motor function following dopamine depletion may be due to the loss of LTD in indirect-pathway MSNs, which normally requires dopamine D2 receptor activation (Kreitzer and Malenka, 2007). Therefore, we next tested whether LTD could be elicited in indirect-pathway MSNs from dopamine-depleted RGS4$^{-/-}$ mice, where activation of the dopamine D2 receptor is not required for LTD (Fig. 6B). We observed normal indirect-pathway HFS-LTD after dopamine depletion with 6-OHDA in RGS4$^{-/-}$ mice (57 $\pm$ 10% of baseline at 30-40 min), whereas in wildtype mice HFS-LTD was absent (97 $\pm$ 11% of baseline at 30-40 min; $p<0.05$ compared to RGS4$^{-/-}$; Fig. 6E). This finding also held true for LFS-LTD (70 $\pm$ 10% of baseline at 30-40 min for RGS4$^{-/-}$ mice vs. 90 $\pm$ 5% of baseline at 30-40 min for wildtype mice; $p<0.05$; Supp. Fig. 1B).

RGS4$^{-/-}$ mice exhibit fewer behavioral deficits in a mouse model of Parkinson's disease

Loss of indirect-pathway LTD may be a key factor in the overactivity of the indirect pathway—and the concomitant reduction in motor activity—observed after loss of striatal dopamine innervation (DeLong and Wichmann, 2007; Filion and Tremblay, 1991; Obeso et al., 2000). Because RGS4$^{-/-}$ indirect-pathway MSNs, unlike wildtype indirect-pathway MSNs, retain the ability to undergo LTD in dopamine-depleted conditions, we reasoned that RGS4$^{-/-}$ mice might have fewer behavioral deficits following dopamine depletion. To test this hypothesis, we unilaterally injected 6-OHDA into the medial forebrain bundle of RGS4$^{-/-}$ and wildtype mice (Fig. 7A). A subset of mice (of each genotype) was injected with an equivalent volume of saline as a control. One week after the injections, each mouse was placed in an open field chamber for 10 minutes and its movement was monitored using video tracking software. Wildtype mice injected with 6-OHDA had clear movement deficits when compared to their saline-injected counterparts (Fig. 7B-F). Overall, they moved less distance during the 10-minute test period (2015 $\pm$ 178 cm for saline-injected wildtype mice vs. 981 $\pm$ 178 cm for 6-OHDA-injected wildtype mice; $p<0.05$). In contrast, RGS4$^{-/-}$ mice treated with 6-OHDA, traveled the same distance as their saline-injected counterparts (2075 $\pm$ 85 cm for saline-injected RGS4$^{-/-}$ mice vs. 1618 $\pm$ 293 cm for 6-OHDA-injected RGS4$^{-/-}$ mice). RGS4$^{-/-}$ mice treated with 6-OHDA also traveled significantly more distance than wildtype mice treated with 6-OHDA (Fig. 7C).

To further dissect the changes in movement that occurred following 6-OHDA injection, we analyzed the percentage of time each mouse spent motionless, ambulating,

or making fine movements such as grooming. Wildtype mice that were injected with 6-OHDA spent less time ambulating and more time motionless than wildtype mice injected with saline. In contrast, RGS4$^{-/-}$ mice were resistant to the motor deficits displayed by wildtype mice (34 ± 3% of time spent making fine movements, 56 ± 1% ambulating, 10 ± 2% freezing for saline-injected wildtype mice; 22 ± 4% of time spent making fine movements, 27 ± 7% ambulating, 51 ± 11% freezing for 6-OHDA-injected wildtype mice; 25 ± 0.4% of time spent making fine movements, 57 ± 1% ambulating, 18 ± 1% freezing for saline-injected RGS4$^{-/-}$ mice; 23 ± 1% of time spent making fine movements, 50 ± 7% ambulating, 27 ± 7% freezing for 6-OHDA-injected RGS4$^{-/-}$ mice; Fig. 7D). RGS4$^{-/-}$ mice were also resistant to deficits observed in wildtype mice in ambulation velocity (5.57 ± 0.44 cm/s for saline-injected wildtype mice; 3.69 ± 0.37 cm/s for 6-OHDA-injected wildtype mice; 5.27 ± 0.22 cm/s for saline-injected RGS4$^{-/-}$ mice; 5.10 ± 0.41 cm/s for 6-OHDA-injected RGS4$^{-/-}$ mice; Fig. 7E) and ambulation bout length (1.60 ± 0.07 s for saline-injected wildtype mice; 1.19 ± 0.12 s for 6-OHDA-injected wildtype mice; 1.83 ± 0.08 s for saline-injected RGS4$^{-/-}$ mice; 1.63 ± 0.19 s for 6-OHDA-injected RGS4$^{-/-}$ mice; Fig. 7F).

Notably, despite the fact that the open field behavior of unilaterally 6-OHDA-injected RGS4$^{-/-}$ mice was largely, though not fully, intact, we observed that unilaterally 6-OHDA-injected RGS4$^{-/-}$ and wildtype mice had similar ipsilateral rotational biases (Supp. Fig. 5). This result was surprising given the other behavioral phenotypes that are improved in the 6-OHDA-injected RGS4$^{-/-}$ mice. However, the role of dopamine in the striatum extends beyond the regulation of synaptic plasticity and thus, despite improvements in behavioral deficits in 6-OHDA-injected RGS4$^{-/-}$ mice, these mice probably still have significant imbalances in the function of the contralateral and ipsilateral striatum, which could lead to rotational behavior. The mechanistic origin of

rotational behavior following dopamine depletion is not well understood so it is difficult to speculate further.

We also tested whether RGS4 deficiency could rescue behavioral deficits caused by injection of 6-OHDA to both sides of the striatum (Supp. Fig. 6A). Bilateral injection of 6-OHDA caused more severe behavioral deficits than unilateral injection, but the overall differences between wildtype and RGS4$^{-/-}$ mice were quite similar. Four days after 6-OHDA injection (the longest we could consistently keep these mice alive), wildtype mice had drastically decreased their total distance traveled and time spent ambulating, and drastically increased their time spent freezing (Supp. Fig. 6B, C). In contrast, RGS4$^{-/-}$ mice did not decrease their total distance traveled (Supp. Fig. 6B). RGS4$^{-/-}$ mice did significantly decrease their time spent ambulating and increase their time spent freezing in this test; however, their behavioral deficits were significantly less severe than wildtype mice (Supp. Fig. 6C). As we observed in unilaterally injected mice, bilaterally 6-OHDA-injected RGS4$^{-/-}$ mice were resistant to deficits observed in bilaterally 6-OHDA-injected wildtype mice in ambulation velocity (Supp. Fig. 6D)

The results of our open field experiments were striking, however, movement in an open field does not require any motor coordination or skill. We therefore decided to test whether motor coordination deficits following dopamine depletion with 6-OHDA could also be improved in RGS4$^{-/-}$ mice in comparison to wildtypes. For these experiments, we used unilateral 6-OHDA injections since the decreased severity of the freezing phenotype in these mice allowed us to better assess coordination. To test for motor coordination, we used a balance beam task in which mice must traverse a narrow, elevated beam to reach a dark, enclosed box. Each mouse was tested on three trials and foot slips on the beam as well as falls off the beam were counted for each trial. Saline-injected wildtype and RGS4$^{-/-}$ mice both appeared similarly coordinated on this

task; they made very few foot slips and almost never fell off the beam (0.67 ± 0.11 slips and 0.07 ± 0.05 falls per trial for wildtype mice, 0.89 ± 0.09 slips and 0.03 ± 0.04 falls per trial for RGS4$^{-/-}$ mice; Fig.7G, H). 6-OHDA-injected wildtype mice, however, were impaired. Of nine mice tested, three could not perform the task at all. The six mice that did traverse the beam had more foot slips and also fell off the beam significantly more than their saline-injected counterparts (1.59 ± 0.36 slips and 1.67 ± 0.59 falls per trial; Fig. 7H). They usually fell at least once and often more than once per trial, meaning they could not have completed the task without being placed back onto the beam by the experimenter. In contrast, 6-OHDA-injected RGS4$^{-/-}$ mice almost never slipped or fell on the balance beam (0.33 ± 0.08 slips and 0.09 ± 0.06 falls per trial; Fig. 7H). There were no significant differences in slipping or falling between 6-OHDA-injected RGS4$^{-/-}$ mice and their saline-injected counterparts and indeed, 6-OHDA-injected RGS4$^{-/-}$ mice performed significantly better than 6-OHDA-injected wildtype mice. These data indicate that RGS4$^{-/-}$ mice are significantly more coordinated following dopamine depletion than wildtype mice. Furthermore, our open field and balance beam data all support the conclusion that RGS4 is a critical link between loss of dopamine, dysregulation of striatal eCB-LTD, and motor impairments.

Discussion

In this study, we characterized a novel mechanism linking dopamine D2 and adenosine A2A receptor signaling to mobilization of eCBs through the GTPase-accelerating protein RGS4. We found that eCB-LTD can be induced by engaging either of two distinct biosynthetic pathways, both of which require D2 receptor activation and are inhibited by A2A receptor activation. This modulation of eCB-LTD by D2 and A2A receptors requires RGS4, which is phosphorylated by PKA (Huang et al., 2007) and inhibits mGluR-G_q signaling (Saugstad et al., 1998). RGS4 is therefore a key link between dopamine signaling, synaptic plasticity, and motor behavior, and may be a promising non-dopaminergic target for modulating basal ganglia circuitry.

Two distinct forms of indirect-pathway eCB-LTD

Our finding of two distinct forms of eCB-LTD (HFS-LTD and LFS-LTD) in the same cell type both clarifies previous findings and raises new questions. Our data agree with previous studies indicating that AEA is the endocannabinoid mediating HFS-LTD while highlighting the importance of PLD for its production (Ade and Lovinger, 2007; Kreitzer and Malenka, 2007). However, other studies of striatal eCB-LTD have indicated that 2-AG is the endocannabinoid that mediates striatal eCB-LTD (Fino et al., 2010; Lerner et al., 2010). Indeed, we confirm that 2-AG can also mediate eCB-LTD, given the right stimulation frequency and duration, thus helping to resolve some of the apparent conflicts in the literature. Additionally, our LFS-LTD data fit well with a previous study of striatal LTD using low-frequency stimulation (Ronesi and Lovinger, 2005), which until now was difficult to reconcile with studies of HFS-LTD. Like this LTD, which was induced by 5 minutes of continuous 10 Hz stimulation, our LFS-LTD is prevented by blockers of

CB1 receptors and D2 receptors, but not by L-VGCC blockers or by calcium chelation with BAPTA. Together with our own data, these findings demonstrate that eCB-LTD can be calcium-independent, most likely because PLCβ can be sufficiently activated by prolonged group I mGluR activation alone.

The fact that these two forms of eCB-LTD co-exist in the same cell begs the question: why are there two distinct signaling pathways mediating eCB production, and under what types of conditions are they engaged *in vivo*? Discovering the true answer to this question clearly requires further study. There is good evidence for both AEA and 2-AG release in the striatum *in vivo* after administration of drugs that alter D2 and A2A receptor signaling (Giuffrida et al., 1999; Lerner et al., 2010). We speculate that the release of eCBs in response to different types of afferent activity may be important for responding to different types of signals in the environment, however, the nature of those environmental signals and their relation to eCB mobilization have yet to be determined. The pathway engaged by HFS-LTD appears well-suited for responding to brief intense stimuli and would likely require synchronous excitatory input to the striatum such as might occur normally during periods of learning or focused attention (Murthy and Fetz, 1992; Steinmetz et al., 2000), as well as during damaging excitotoxic processes (Hansen et al., 2001). Meanwhile, the pathway engaged by LFS-LTD requires less intense stimulation, which might not require such synchronous excitatory input to occur *in vivo*. However, this pathway must be engaged for longer periods of time (both our LFS-LTD protocol and Ronesi and Lovinger's protocol lasted 5 min overall, compared with less than 1 minute for the HFS-LTD protocol), or must be enhanced by neuromodulators, in order for transient depression to be consolidated into LTD (Lerner et al., 2010; Ronesi and Lovinger, 2005; Uchigashima et al., 2007).

Why aren't both AEA and 2-AG released during our HFS- and LFS-LTD protocols? In the case of LFS-LTD, the answer may be simple – LFS may not yield

strong depolarization of the distal dendrites, which could limit the activation of L-VGCCs required for AEA production. But why isn't 2-AG released during HFS-LTD? We suggest several possibilities, which are not mutually exclusive. First, the release of AEA can inhibit the mobilization of 2-AG (Maccarrone et al., 2008). Second, the engagement of the mGluR-G_q-Src pathway may come at the exclusion of the mGluR-G_q-PLC pathway. Third, 2-AG may actually be released, but it doesn't bind to CB1 receptors long enough to induce presynaptic LTD. 2-AG is a full agonist of CB1 receptors, but has lower affinity for CB1 than AEA, which is a high-affinity partial agonist. Thus, for 2-AG to induce LTD, it may need to be released over several minutes.

Dopamine D2 and adenosine A2A receptors in the postsynaptic neuron modulate LTD induction

Both HFS-LTD and LFS-LTD are modulated by dopamine D2 receptors and adenosine A2A receptors and this modulation of LTD appears to be important for regulating motor function (Kreitzer and Malenka, 2007; Lerner et al., 2010). Here we provide the first evidence of a specific mechanism by which D2 and A2A receptor modulation of LTD occurs. D2 and A2A receptors regulate cAMP/PKA activity. If cAMP/PKA activity is high, RGS4 is phosphorylated and inhibits G_q, preventing LTD. If cAMP/PKA activity is low, RGS4 is not phosphorylated and G_q is able to function to induce LTD.

While our experiments argue that D2 and A2A receptors regulate LTD induction mainly via their downstream signaling pathways, we cannot rule out a role for physical interactions of D2 and A2A receptors in the membrane, which have been reported (for review see Fuxe et al., 2005; Fuxe et al., 2007), though not studied in the context of LTD. Although we see no evidence for the engagement of alternative signaling pathways

through a heteromeric complex in our experiments, D2/A2A heteromerization could, for example, ensure close proximity of these receptors, which would allow them to more precisely coordinate cAMP levels. One thought-provoking study showed that dopamine terminals themselves transiently release adenosine *in vivo* after high-frequency (60 Hz for 1 s) stimulation, but on a slower time scale than dopamine is released (Cechova and Venton, 2008). Activation of A2A receptors by this delayed efflux could help to restrict the window for LTD induction following a burst of dopamine neuron firing, but A2A receptors would need to be located with D2 receptors at the dopamine synapses to take advantage of this possibility.

D2 and A2A receptors appear to regulate cAMP accumulation in MSNs primarily by acting on adenylyl cyclase 5 (AC5), a striatal-enriched form of adenylyl cyclase. Mice lacking AC5 have impaired striatal synaptic plasticity. Specifically, although excitatory synapses onto MSNs from $AC5^{-/-}$ mice respond normally to the group I mGluR agonist DHPG, this response cannot be enhanced by D2 receptor activation as it can in wildtype mice (Kheirbek et al., 2009).

Cyclic AMP/PKA signaling is often subject to additional levels of regulation not examined here, which may play an important role in regulating striatal eCB-LTD. For example, phosphodiesterases (PDEs) control cAMP accumulation by degrading cAMP. PDE10A is a striatal-enriched PDE that has been shown to strongly influence D2 and A2A receptor-dependent phosphorylation of DARPP-32, and likely many other targets, in indirect-pathway MSNs (Nishi et al., 2008). Additionally, targets of PKA phosphorylation, including RGS4, may be subject to active dephosphorylation by phosphatases. Future studies will help to clarify which, if any, of these mechanisms of regulation are critical for the modulation of eCB-LTD.

Some controversy exists in the literature regarding the site of the D2 and A2A receptors that control endocannabinoid release and LTD (Tozzi et al., 2011; Wang et al.,

2006). Importantly, our experiments demonstrate that D2 and A2A receptors exert their action in the postsynaptic neuron. All of the drugs we used to manipulate cAMP/PKA activity are membrane-impermeable and were delivered only to the postsynaptic neuron via the recording pipette. We also delivered both CCG-63802, the RGS4 inhibitor, and recombinant RGS4 protein to the patched postsynaptic neuron via the recording pipette. Thus, we conclude that RGS4 acts cell-autonomously in the postsynaptic neuron and not via an action in neighboring MSNs or interneurons, or in the presynaptic axons.

RGS4 and Disease

Regulators of G-protein signaling (RGSs) are GTPase-activating proteins, which negatively regulate G proteins by accelerating their inactivation. RGS4 is an RGS that is highly expressed in striatum (Gold et al., 1997) and there is evidence linking changes in RGS4 function with a variety of diseases involving the striatum. RGS4 is downregulated in human striatal tissue from Huntington's disease and Parkinson's disease patients, as well as in animal models of these diseases (Geurts et al., 2003; Kuhn et al., 2007; Zhang et al., 2005). It is also downregulated by chronic cocaine and amphetamine treatment, suggesting a role in drug addiction (Schwendt et al., 2007; Schwendt and McGinty, 2007). Human genetic studies have identified RGS4 as a schizophrenia susceptibility gene, however, $RGS4^{-/-}$ mice do not display obvious schizophrenic phenotypes (Grillet et al., 2005). Finally, a recent paper showed that crossing $RGS4^{-/-}$ mice into a mouse model of Fragile X syndrome alleviated many of the symptoms of the disease (Pacey et al., 2011).

Here, we find that $RGS4^{-/-}$ mice have dopamine-independent indirect-pathway eCB-LTD and show fewer behavioral deficits following dopamine depletion with 6-OHDA, a mouse model of Parkinson's disease. This finding suggests that dysregulation

of eCB-LTD is critical for the emergence of parkinsonian motor deficits. If indirect-pathway eCB-LTD can continue to take place in RGS4$^{-/-}$ mice following dopamine depletion, they may be more able than wildtype mice to compensate for the loss of dopamine through adaptive changes in synaptic strength. Loss of RGS4 in direct-pathway MSNs may also be contributing to the improved phenotype of RGS4$^{-/-}$ mice following dopamine depletion since RGS4 is expressed in MSNs of both pathways (Taymans et al., 2004). Although we focused on dissecting the mechanisms underlying indirect-pathway LTD in this paper, Parkinson's disease has been conceptualized as an imbalance between the direct and indirect pathways, meaning that a better understanding of how RGS4 functions in the direct pathway will be an important topic for future study.

RGS4 may play an additional role in Parkinson's disease by regulating acetylcholine M4 receptors on striatal cholinergic interneurons. Although RGS4 is downregulated in dopamine-depleted striatal tissue as a whole, it is upregulated in cholinergic interneurons following dopamine depletion. In these interneurons, RGS4 upregulation inhibits coupling of M4 receptors to Ca_v2 calcium channels, causing a loss of cholinergic autoinhibition and thus increasing cholinergic tone (Ding et al., 2006). RGS4 inhibition could thus help to normalize cholinergic tone in Parkinson's disease in addition to its effects on D2 and A2A receptor signaling.

The reduced behavioral deficits following dopamine depletion in RGS4$^{-/-}$ mice indicate that RGS4 inhibition may be an effective non-dopaminergic strategy for treating Parkinson's disease. Although downregulation of RGS4 may be an adaptive change that already takes place in response to dopamine depletion to some degree (Geurts et al., 2003; Zhang et al., 2005), our findings indicate that further downregulation is beneficial. In this study, we were able to use an existing compound, CCG-63802, at a relatively high concentration (100 μM) delivered directly to single neurons via the intracellular

recording solution to inhibit RGS4 activity. Although helpful for our study, administration of CCG-63802 or related analogs *in vivo* is not likely to be an effective strategy, due to the sensitivity of these compounds to reducing conditions (Blazer et al., 2011). Potentially, RGS4 inhibitors with suitable characteristics for clinical use are on the horizon and can be tested as Parkinson's disease therapeutics. Such compounds could also prove to be useful treatments for other conditions in which RGS4 is involved, such as Huntington's disease, drug addiction, schizophrenia, and Fragile X syndrome.

Acknowledgements

We thank Ron Taussig, Todd Golde, Carolina Ceballos, Yao Chen, Bernardo Sabatini, Steve Finkbeiner, Eva LaDow, Erica Korb, Liza Shoenfeld, Nora Hammack, Alexxai Kravitz, Giao Hang, and other members of the Kreitzer Lab for providing helpful advice on experiments, comments on the manuscript, technical assistance, and reagents. We also thank Nino Devidze and Brittany Masatsugu of the Gladstone Institutes' Behavioral Core for help obtaining the behavioral data. This work was supported by NIH R01 NS064984, the Pew Biomedical Scholars Program, the W.M. Keck Foundation, and the McKnight Foundation.

Figures

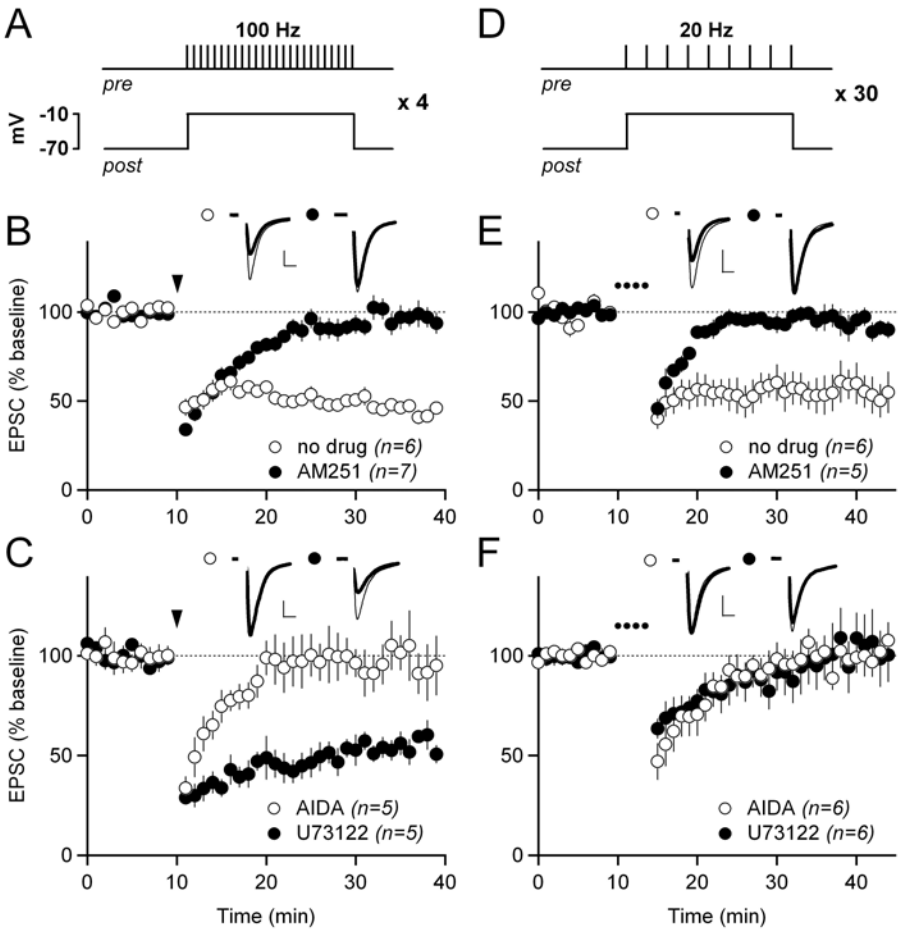

Figure 1. PLCβ-dependent and -independent forms of eCB-LTD can be elicited at excitatory synapses onto striatal indirect-pathway MSNs.

(A) Schematic of the high-frequency stimulation (HFS)-LTD induction protocol. 100 Hz stimulation for one second was paired with postsynaptic depolarization to -10 mV. This stimulation was repeated four times at ten second intervals.

(B) HFS-LTD in control conditions (white circles) and in 1 μM of the CB1R antagonist AM251 (black circles). In this and all subsequent panels showing LTD, normalized EPSC amplitudes are plotted over time. Traces from representative experiments are shown above the graph. The thin traces show the average

EPSC from 0-10 minutes, and the thick traces show the average EPSC from 30-40 minutes. For HFS-LTD, the arrowhead indicates the time of induction. In all panels, scale bars are 100 pA x 5 ms and error bars are SEM.

(C) HFS-LTD in 100 μM of the mGluR1/5 antagonist AIDA (white circles), and with 10 μM of the PLCβ inhibitor U73122 included in the intracellular pipette solution (black circles).

(D) Schematic of the low-frequency stimulation (LFS)-LTD induction protocol. 20 Hz stimulation for one second was paired with postsynaptic depolarization to -10 mV. This stimulation was repeated 30 times at ten second intervals to induce LFS-LTD.

(E) LFS-LTD in control solution (white circles) and in 5 μM AM251 (black circles). In all panels showing LFS-LTD, the dotted line indicates the time of LFS-LTD induction.

(F) LFS-LTD in 100 μM AIDA (white circles) and with 10 μM U73122 included in the intracellular solution (black circles).

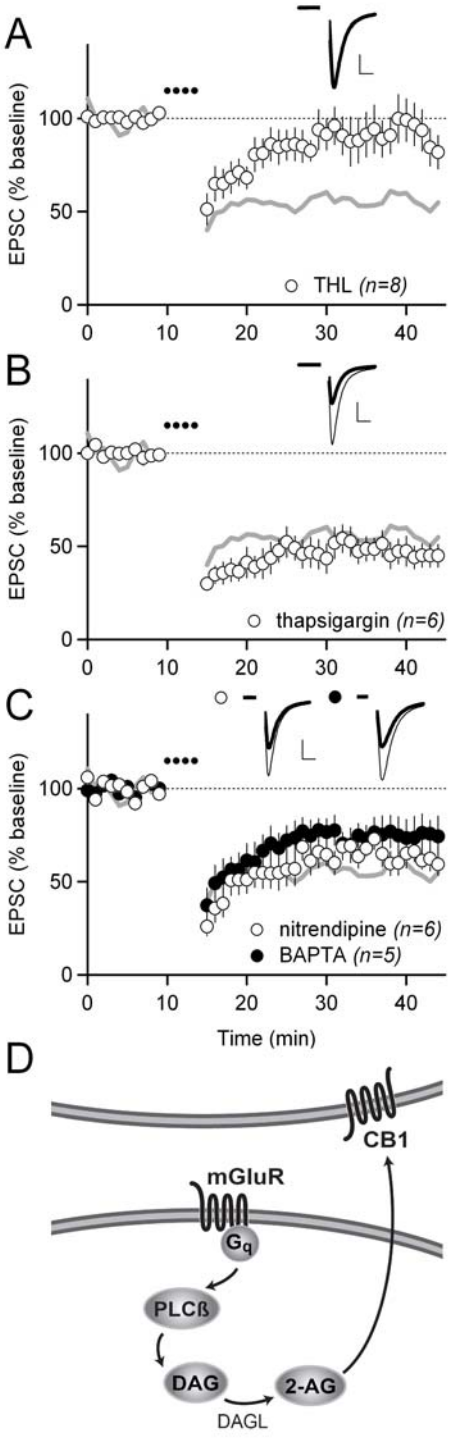

Figure 2. LFS-LTD requires diacylglycerol lipase, but not elevations in intracellular calcium.

(A) LFS-LTD in 10 μM of the diacylglycerol lipase inhibitor THL. Gray traces in A, B, and C show control LFS-LTD from Figure 1E for reference. In all panels, scale bars are 100 pA x 5 ms and error bars are SEM.

(B) LFS-LTD with 10 μM of the intracellular calcium store depleter thapsigargin included in the intracellular solution.

(C) LFS-LTD with 10 μM of the L-type calcium channel blocker nitrendipine (white circles), and with 10 μM of the calcium chelator BAPTA (black circles) included in the intracellular solution.

(D) Schematic showing the proposed signaling pathway underlying LFS-LTD. Activation of G_q-coupled mGluRs activates PLCβ, stimulating the production of diacylglycerol (DAG), which is then converted to the endocannabinoid 2-arachidonoylglycerol (2-AG) by diacylglycerol lipase (DAGL).

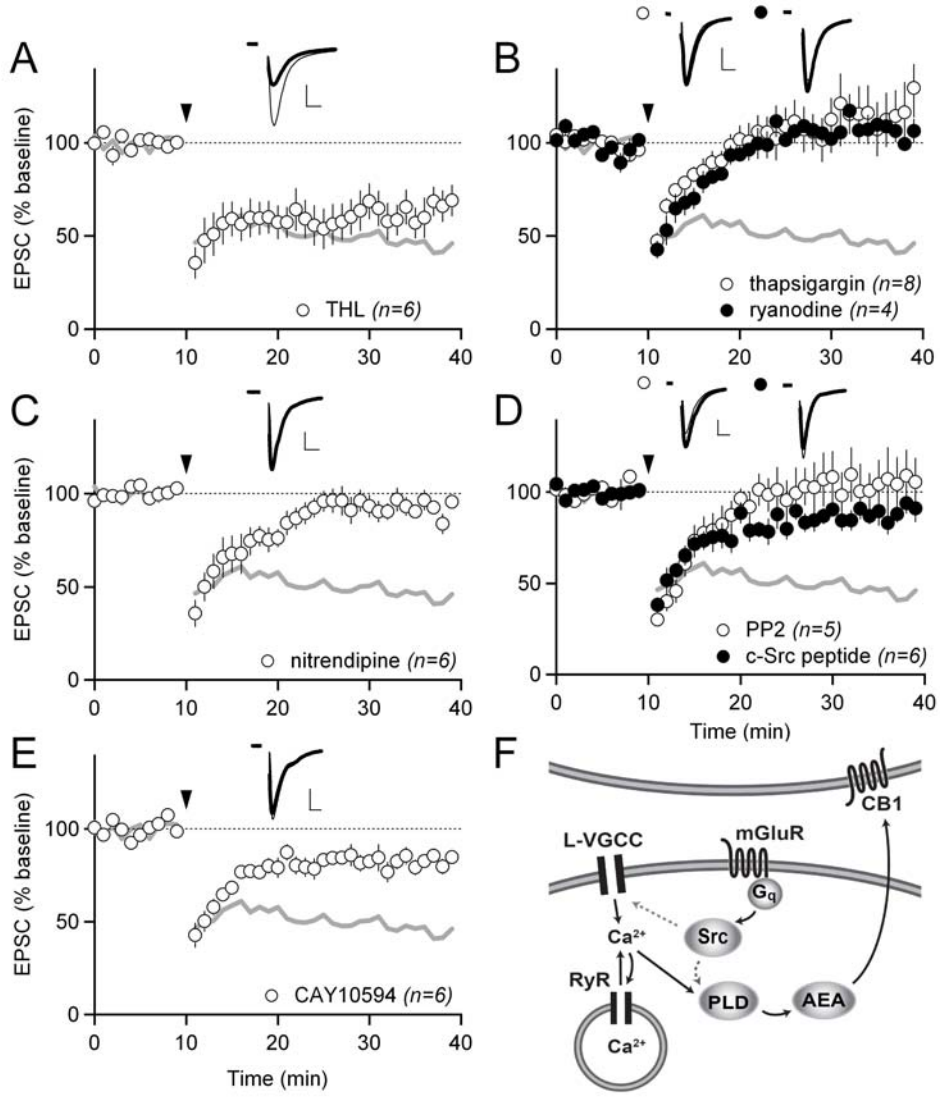

Figure 3. HFS-LTD depends on a distinct signaling pathway involving Src kinase, internal calcium stores, L-type calcium channels, and phospholipase D.

(A) HFS-LTD in 10 μM of the diacylglycerol lipase inhibitor THL. Gray traces in A-E show control HFS-LTD from Figure 1B for reference. In all panels, scale bars are 100 pA x 5 ms and error bars are SEM.

(B) HFS-LTD with 10 μM of the intracellular calcium store depleter thapsigargin included in the intracellular solution (white circles) and with 10 μM ryanodine

included in the intracellular solution to specifically block ryanodine receptors (black circles).

(C) HFS-LTD in 10 μM of the L-type calcium channel blocker nitrendipine.

(D) HFS-LTD in 10 μM of the Src-family kinase inhibitor PP2 (white circles), and with 100 μM c-Src inhibitory peptide included in the intracellular solution (black circles).

(E) HFS-LTD with 100 μM of the phospholipase D (PLD) inhibitor CAY10594 (white circles).

(F) Schematic showing the proposed signaling pathway underlying HFS-LTD. Activation of G_q-coupled mGluRs activates Src, which phosphorylates and activates L-type calcium channels and/or PLD. Calcium influx through L-type calcium channels (amplified by RyR-mediated calcium-induced calcium release from internal stores) also activates PLD. PLD activity leads to the production and release of the endocannabinoid anandamide (AEA).

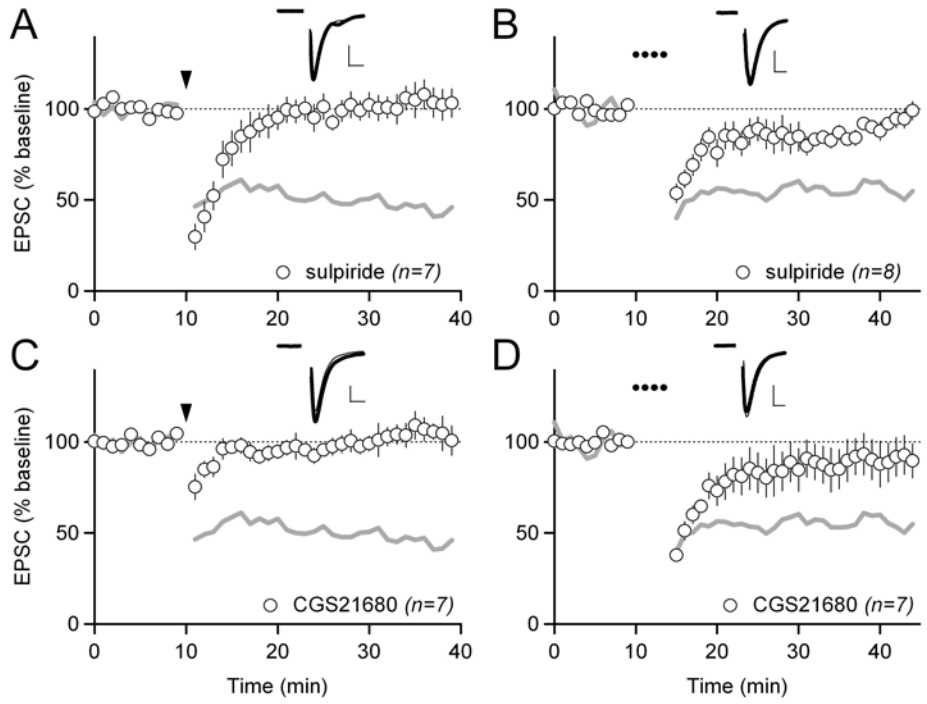

Figure 4. Dopamine D2 and adenosine A2A receptors modulate both LFS- and HFS-LTD.

(A) HFS-LTD in 1 μM of the dopamine D2 receptor antagonist sulpiride. Gray traces in A and C show control HFS-LTD from Figure 1B for reference. In all panels, scale bars are 100 pA x 5 ms and error bars are SEM.

(B) LFS-LTD in 1 μM sulpiride. Gray traces in B and D show control LFS-LTD from Figure 1E for reference.

(C) HFS-LTD in 1 μM of the adenosine A2A receptor agonist CGS21680.

(D) LFS-LTD in 1 μM CGS21680.

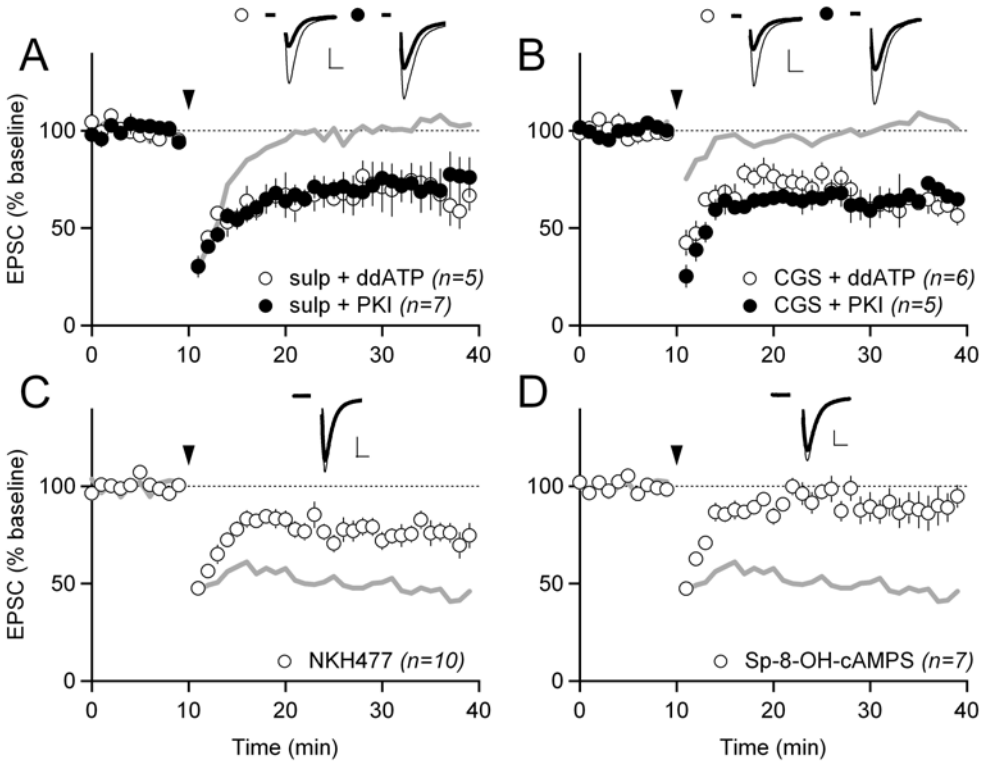

Figure 5. D2 and A2A receptors modulate LTD through cAMP/PKA signaling.

(A) HFS-LTD in 1 μM of the D2 receptor antagonist sulpiride and with either 500 nM of the adenylyl cyclase inhibitor ddATP (white circles) or 100 μM of the PKA inhibitor PKI (black circles) in the intracellular solution. Gray trace shows HFS-LTD in sulpiride with no drug in the intracellular solution from Figure 4A for reference. In all panels, scale bars are 100 pA x 5 ms and error bars are SEM.

(B) HFS-LTD in 1 μM of the A2A receptor agonist CGS21680 and with either 500 nM ddATP (white circles) or 100 μM PKI (black circles) in the intracellular solution. Gray trace shows HFS-LTD in CGS21680 with no drug in the intracellular solution from Figure 4C for reference.

(C) HFS-LTD with 10 μM of the adenylyl cyclase activator NKH477 in the intracellular recording solution. Gray traces in C and D show control HFS-LTD from Figure 1B.

(D) HFS-LTD with 0.5-1 mM of the PKA activator Sp-8-OH-cAMPS in the intracellular recording solution.

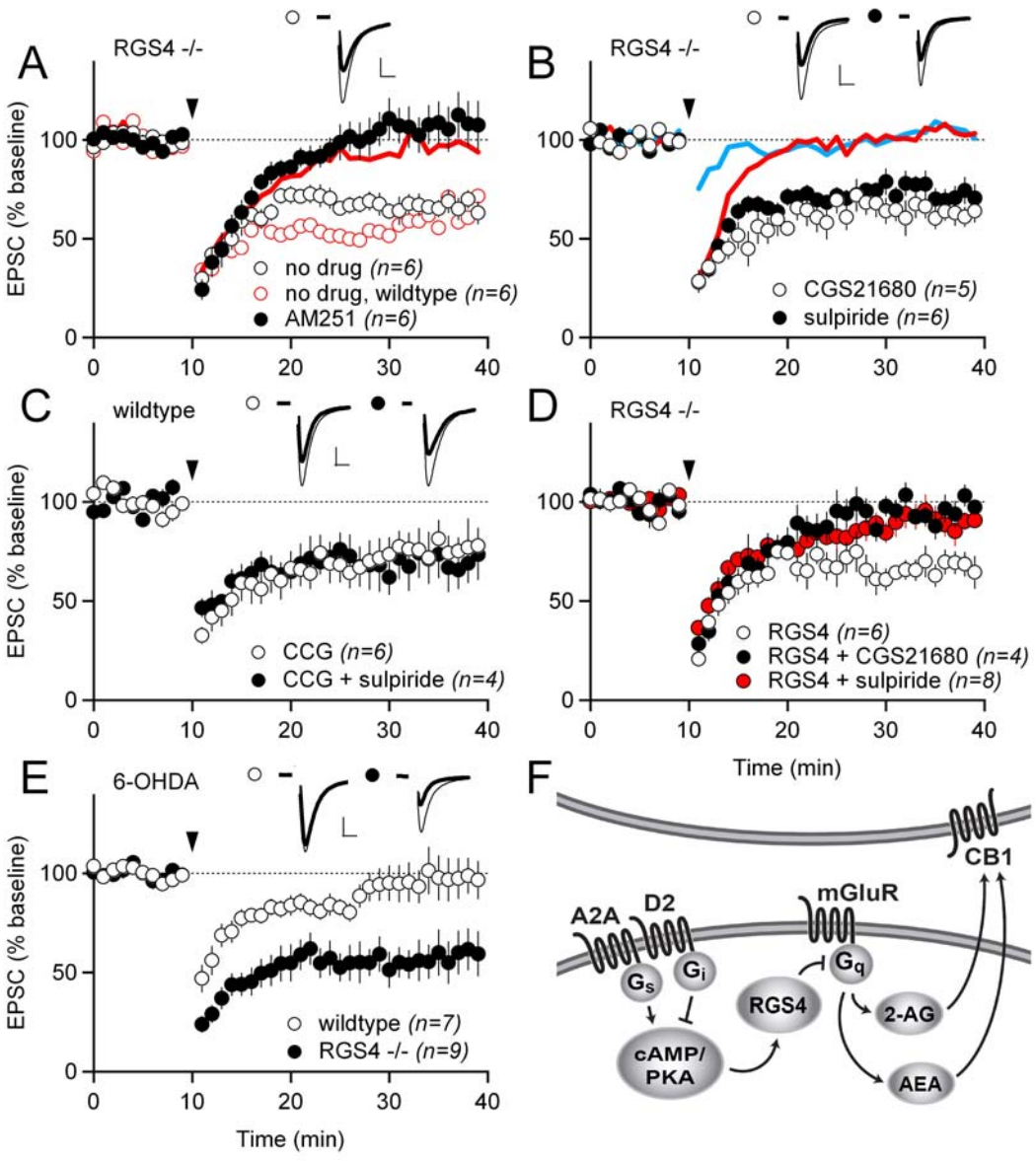

Figure 6. D2 and A2A receptors regulate striatal LTD via regulator of G-protein signaling 4 (RGS4).

(A) HFS-LTD in RGS4$^{-/-}$ mice in control (no drug) solution (white circles) and in 1 μM of the CB1R antagonist AM251 (black circles). Interleaved HFS-LTD experiments in wildtype mice in control solution are shown as open red circles. The blue trace

shows the data from HFS-LTD experiments in wildtype mice in 1 μM AM251 from Figure 1B for reference.

(B) HFS-LTD in RGS4$^{-/-}$ mice in 1 μM of the A2A receptor agonist CGS21680 (white circles) and in 1 μM of the D2 receptor antagonist sulpiride (black circles). The solid lines show HFS-LTD in wildtype mice in 1 μM CGS21680 (blue trace) and in 1 μM sulpiride (red trace) from Figure 4A, C.

(C) HFS-LTD with 100 μM of the RGS4 inhibitor CCG-63802 included in the intracellular solution, in combination with either no drug (white circles) or with 1 μM sulpiride (black circles) in the bath.

(D) HFS-LTD in RGS4$^{-/-}$ mice with 25 pM recombinant RGS4 protein included in the intracellular solution and with either no drug (white circles) or with 1 μM CGS21680 (black circles) or with 1 μM sulpiride (red circles) in the bath.

(E) HFS-LTD in dopamine-depleted slices. Slices are from the treated hemisphere of mice injected unilaterally with 6-OHDA in the medial forebrain bundle. Results are shown for wildtype (white circles) and RGS4$^{-/-}$ mice (black circles).

(F) Schematic showing the proposed signaling pathway by which D2 and A2A receptors modulate eCB-LTD. In this model, D2 and A2A receptors oppositely modulate cAMP/PKA. High PKA activity inhibits mGluR-G_q signaling via RGS4. Inhibition of mGluR-G_q signaling prevents the mobilization of both 2-AG and AEA.

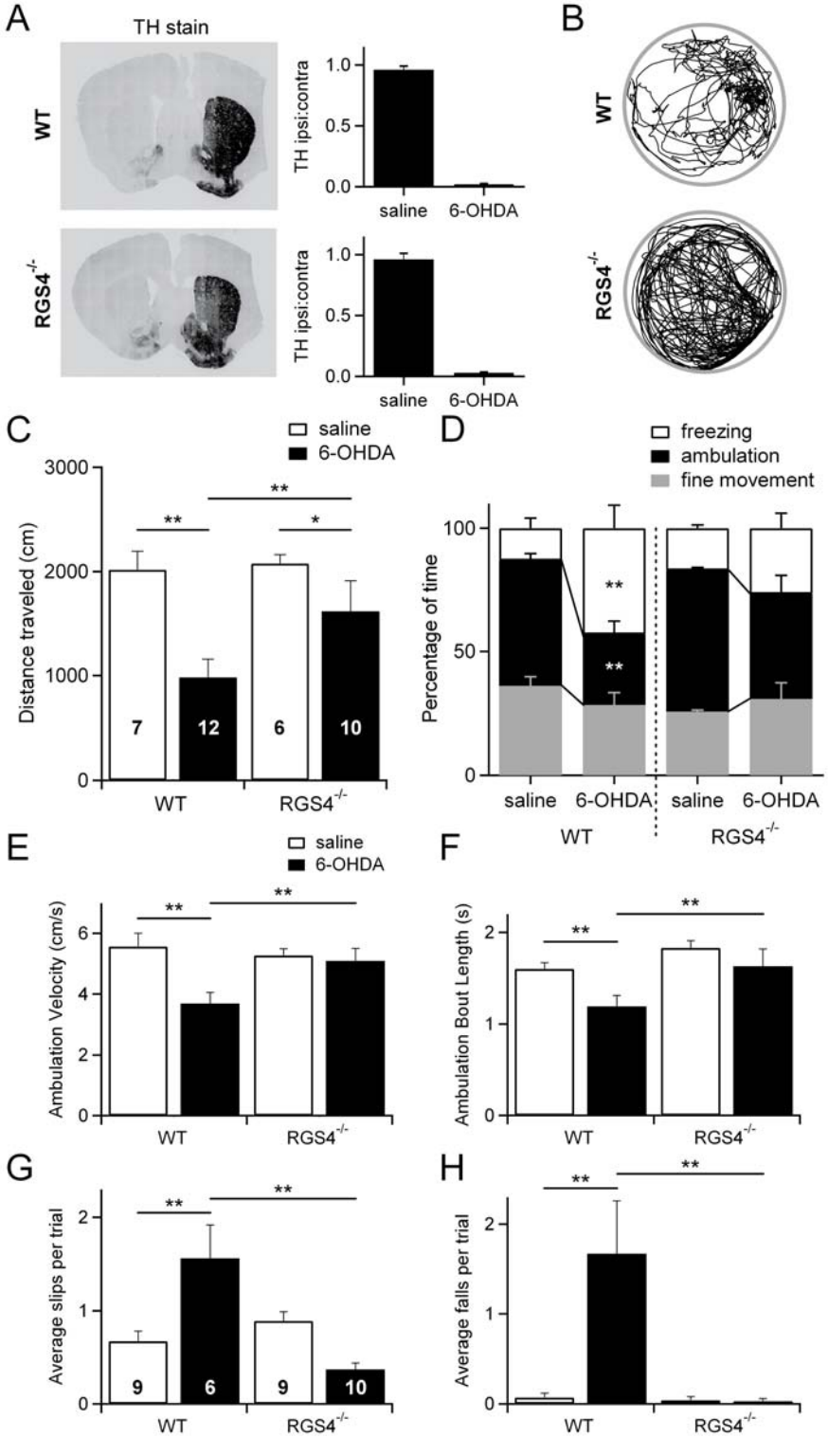
A
TH stain
WT
RGS4-/-
TH ipsi:contra
1.0
0.5
0.0
saline
6-OHDA
B
WT
RGS4-/-
C
saline
6-OHDA
Distance traveled (cm)
3000
2000
1000
0
**
**
*
7
12
6
10
WT
RGS4-/-
D
freezing
ambulation
fine movement
Percentage of time
100
50
0
**
**
saline
6-OHDA
saline
6-OHDA
WT
RGS4-/-
E
saline
6-OHDA
Ambulation Velocity (cm/s)
6
4
2
0
**
**
WT
RGS4-/-
F
Ambulation Bout Length (s)
2
1
0
**
**
WT
RGS4-/-
G
Average slips per trial
2
1
0
**
**
9
6
9
10
WT
RGS4-/-
H
Average falls per trial
2
1
0
**
**
WT
RGS4-/-

Figure 7. RGS4$^{-/-}$ mice have fewer behavioral deficits in a mouse model of Parkinson's disease.

(A) Left, example images of coronal brain slices from wildtype (WT) and RGS4$^{-/-}$ mice stained for tyrosine hydroxylase (TH) to verify dopamine depletion following unilateral 6-OHDA injections. Right, quantification of dopamine depletion in all WT and RGS4$^{-/-}$ mice used for behavioral analysis. The intensity of fluorescence on the ipsilateral side was compared to that on the contralateral side for each mouse to yield the TH ipsi:contra ratio.

(B) Examples of the paths taken by dopamine-depleted WT and RGS4$^{-/-}$ mice during the 10 minute test period. The example paths shown are from the same mice whose TH staining is shown in A.

(C) The distances traveled during the test period are shown for saline-injected WT mice (n=7), 6-OHDA-injected WT mice (n=12), saline-injected RGS4$^{-/-}$ mice (n=6), and 6-OHDA-injected RGS4$^{-/-}$ mice (n=10). Data from the same group of mice is also shown in D, E, and F.

(D) The percentage of time spent freezing, ambulating, or making fine movements is shown for saline-injected WT mice (n=7), 6-OHDA-injected WT mice (n=12), saline-injected RGS4$^{-/-}$ mice (n=6), and 6-OHDA-injected RGS4$^{-/-}$ mice (n=10).

(E) Average velocity during periods of ambulation is shown for saline-injected WT mice (n=7), 6-OHDA-injected WT mice (n=12), saline-injected RGS4$^{-/-}$ mice (n=6), and 6-OHDA-injected RGS4$^{-/-}$ mice (n=10).

(F) Average length of an ambulation bout (time spent continuously ambulating before stopping) is shown for saline-injected WT mice (n=7), 6-OHDA-injected WT mice (n=12), saline-injected RGS4$^{-/-}$ mice (n=6), and 6-OHDA-injected RGS4$^{-/-}$ mice (n=10).

(G) The average number of foot slips per trial on the balance beam is shown for saline-injected WT mice (n=9), 6-OHDA-injected WT mice (n=6), saline-injected RGS4$^{-/-}$ mice (n=9), and 6-OHDA-injected RGS4$^{-/-}$ mice (n=10). Data from the same group of mice is also shown H. Three additional 6-OHDA-injected WT mice were tested on the balance beam, but failed to perform the task.

(H) The average number of falls per trial on the balance beam is shown for saline-injected WT mice (n=9), 6-OHDA-injected WT mice (n=6), saline-injected RGS4$^{-/-}$ mice (n=9), and 6-OHDA-injected RGS4$^{-/-}$ mice (n=10).

*p<0.05; **p<0.01.

Supplementary Figures

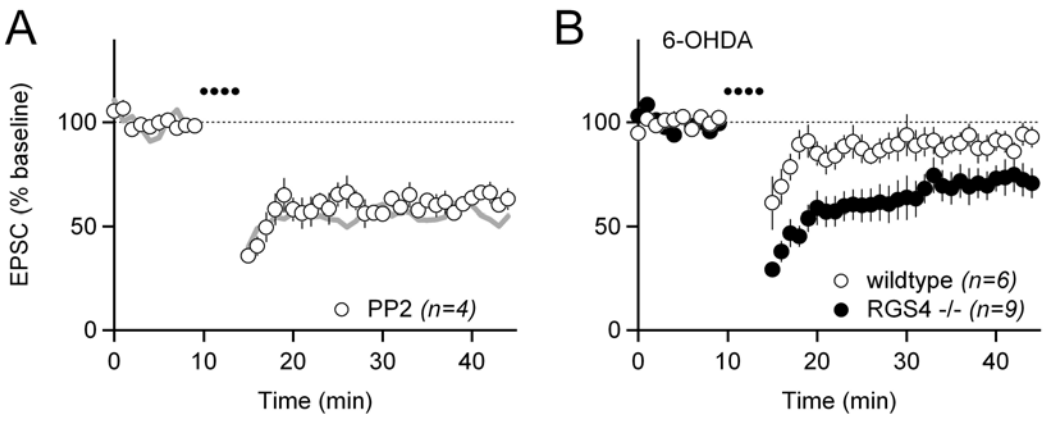

Supplementary Figure 1. Further characterization of LFS-LTD, related to Figure 2

(A) LFS-LTD in 10 μM of the Src-family kinase inhibitor PP2. Gray trace shows control LFS-LTD from Figure 1E for reference.

(B) LFS-LTD in dopamine-depleted slices. Slices are from the treated hemisphere of mice injected unilaterally with 6-OHDA in the medial forebrain bundle. Results are shown for wildtype (white circles) and RGS4$^{-/-}$ mice (black circles).

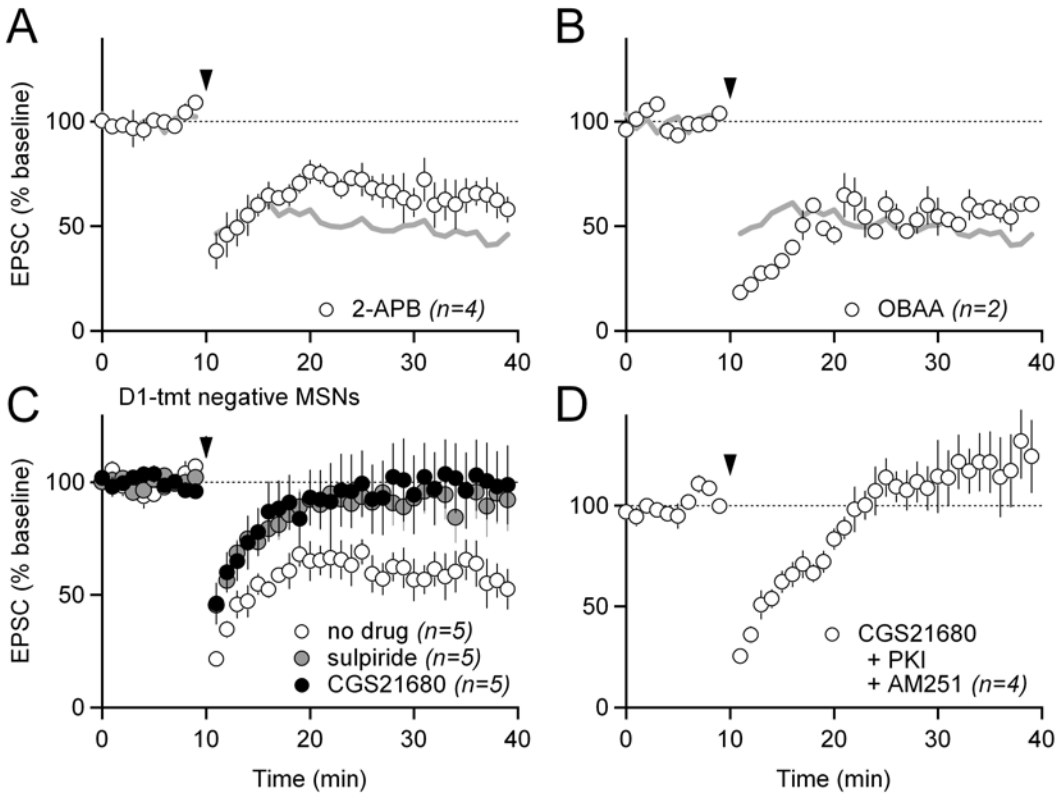

Supplementary Figure 2. Further characterization of HFS-LTD, related to Figure 3

(A) HFS-LTD with 10 μM of the IP_3 receptor inhibitor 2-APB included in the intracellular solution. Gray trace shows control HFS-LTD from Figure 1B for reference.

(B) HFS-LTD in 5 μM of the PLA_2 inhibitor OBAA. Gray trace shows control HFS-LTD from Figure 1B for reference.

(C) HFS-LTD in D1-tmt negative MSNs in control (no drug) solution (white circles) and in 1 μM of the A2AR agonist CGS21680 (black circles) or in 1 μM of the D2R antagonist sulpiride (gray circles).

(D) HFS-LTD in 1 μM of the A2AR agonist CGS21680, with 100 μM of the PKA inhibitor PKI in the intracellular solution and with 1 μM of the CB1R antagonist AM251 added to the bath.

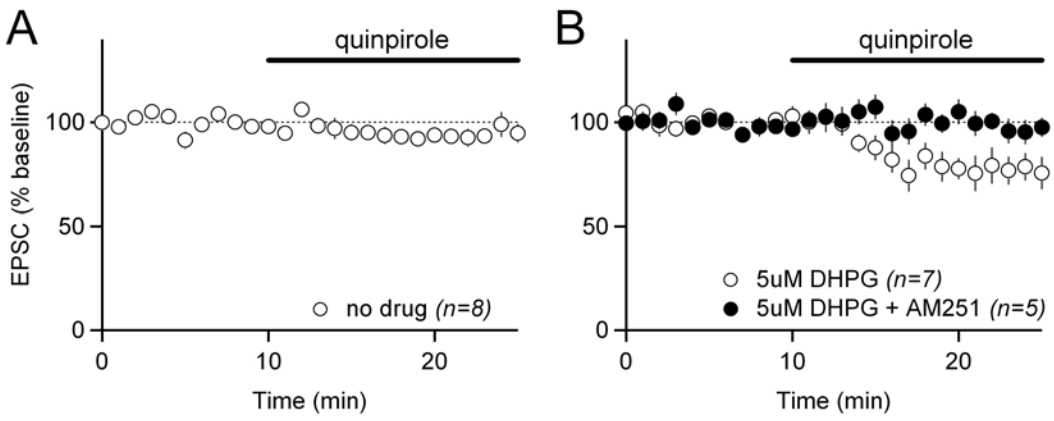

Supplementary Figure 3. Dopamine D2 receptor activation causes endocannabinoid release only when group I mGluRs are already partially activated, related to figure 4

(A) EPSC amplitude following application of the D2R agonist quinpirole. The black horizontal bar indicates the time of quinpirole wash-on.

(B) EPSC amplitude following application of the D2R agonist quinpirole in the presence of a low concentration (5 μM) of the group I mGluR agonist DHPG (white circles) and in the presence of both 5 μM DHPG and 1 μM of the CB1R antagonist AM251 (black circles). The black horizontal bar indicates the time of quinpirole wash-on.

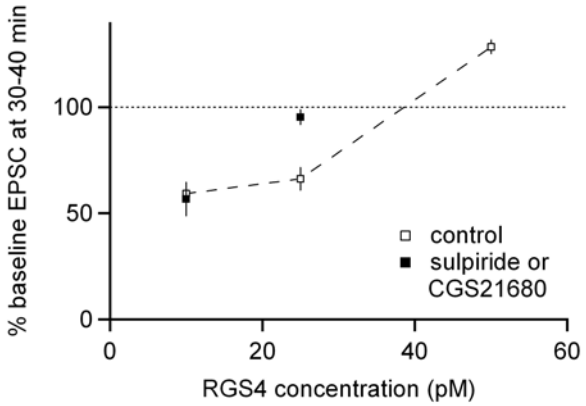

Supplementary Figure 4. Dose-dependence of RGS4 rescue, related to Figure 6

Results (graphed as % of baseline at 30-40 min) of HFS-LTD experiments in RGS4$^{-/-}$ mice with RGS4 recombinant protein included in the intracellular solution. White squares show the results in control extracellular solution at three concentrations of intracellular RGS4: 10 pM (n=2), 25 pM (n=6), and 50 pM (n=2). Black squares show the results in either 1 μM of the A2A agonist CGS21680 or 1 μM of the D2 antagonist sulpiride at the two concentrations of intracellular RGS4 with which LTD could still be induced in control extracellular solution: 10 pm (n=2) and 25 pm (n=12). We did not test the effects of CGS21680 or sulpiride with 50 pM RGS4 protein in the intracellular solution since LTD was already blocked at that concentration of RGS4. All results for 25 pm RGS4 are the same data as those shown in Fig. 6D.

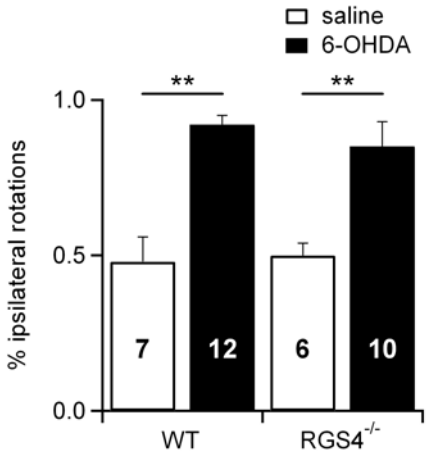

Supplementary Figure 5. Rotation bias in unilaterally dopamine-depleted WT and RGS4$^{-/-}$ mice, related to Figure 7

Percent ipsilateral rotations (ipsilateral rotations divided by total rotations) is shown for saline-injected WT mice (n=7), 6-OHDA-injected WT mice (n=12), saline-injected RGS4$^{-/-}$ mice (n=6), and 6-OHDA-injected RGS4$^{-/-}$ mice (n=10). Data are from the same group of mice shown in Figure 7C, D, E, and F. **p<0.01.

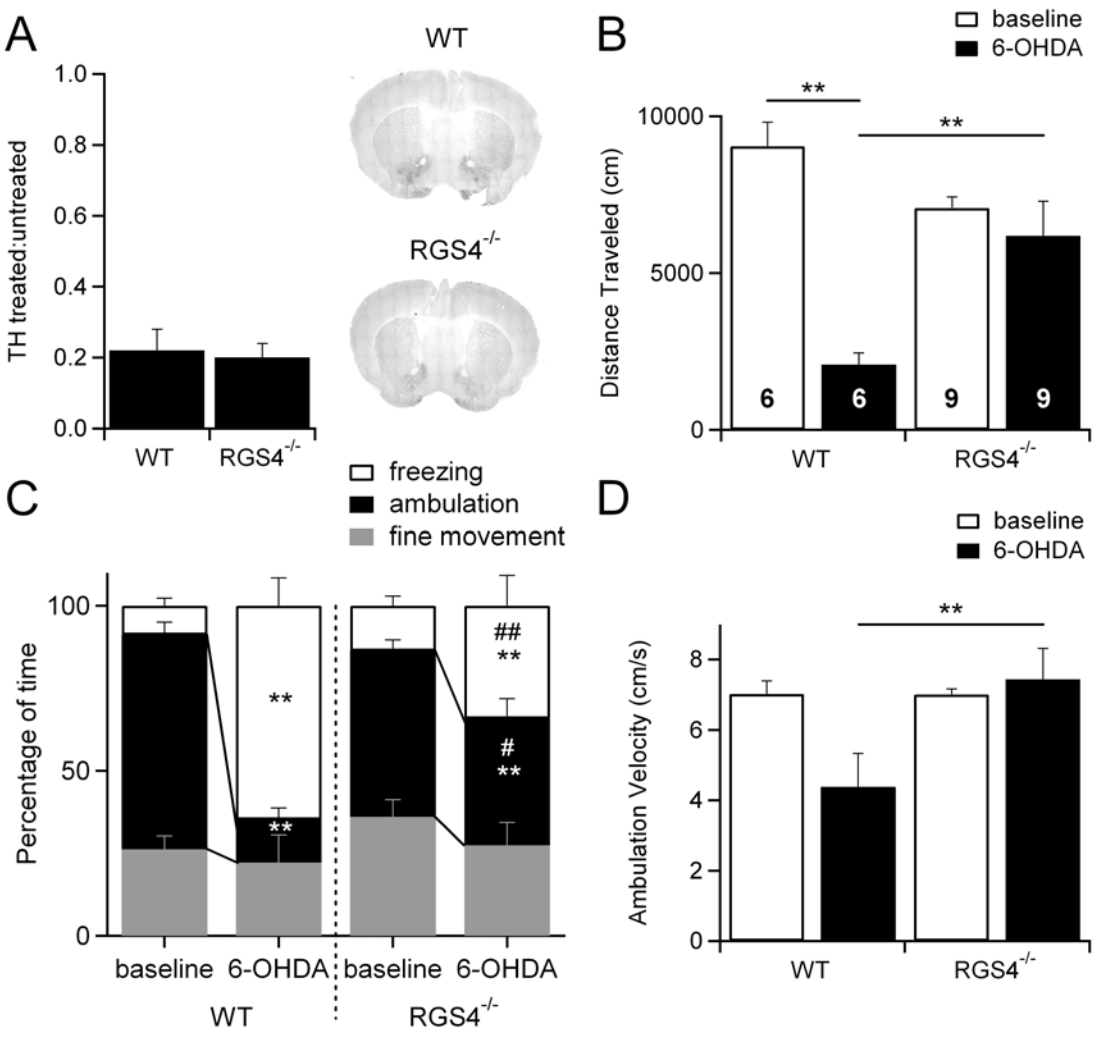

Supplementary Figure 6. RGS4$^{-/-}$ mice have fewer behavioral deficits than wildtype mice following bilateral dopamine depletion, related to Figure 7

(I) Left, quantification of dopamine depletion in all wildtype (WT) and RGS4$^{-/-}$ mice used for behavioral analysis. The average intensity of fluorescence in the two striata of each 6-OHDA-injected mouse was compared to the average intensity of fluorescence in the two striata of an uninjected control mouse of the same genotype to yield the TH treated:untreated ratio. Right, example images of coronal brain slices from WT and RGS4$^{-/-}$ mice stained for tyrosine hydroxylase (TH) to verify dopamine depletion following bilateral 6-OHDA injections.

(J) The distances traveled during a 30-minute test period are shown for WT mice before and after 6-OHDA injection (n=6) and for RGS4$^{-/-}$ mice before and after 6-OHDA injection (n=9). Data from the same group of mice is also shown in C and D. **p<0.01

(K) The percentage of time spent freezing, ambulating, or making fine movements is shown for WT mice before and after 6-OHDA injection (n=6) and for RGS4$^{-/-}$ mice before and after 6-OHDA injection (n=9). **p<0.01 compared to baseline; $^{\#}$p<0.05 compared to 6-OHDA-injected WT mice; $^{\#\#}$p<0.01 compared to 6-OHDA-injected WT mice.

(L) Average velocity during periods of ambulation is shown for WT mice before and after 6-OHDA injection (n=6) and for RGS4$^{-/-}$ mice before and after 6-OHDA injection (n=9). **p<0.01

Chapter 4

Conclusions and Remaining Questions

In this thesis, I have presented data that illuminates our understanding of the mechanisms of endocannabinoid-dependent LTD at excitatory synapses onto indirect-pathway MSNs. Many of the immediate issues raised by my experiments are already considered in the Discussion sections of Chapters 2 and 3. Therefore, in this chapter, I will focus my comments on some of the broader remaining questions in the striatal synaptic plasticity field.

Striatal LTD and LTP: Opponent processes?

Functionally, LTD and LTP are opponent processes, but are the induction of LTD and the induction of LTP linked mechanistically? One attractive hypothesis is that cAMP/PKA signaling links the two processes by oppositely modulating them. Enhanced PKA activity increases NMDA receptor signaling and therefore should promote LTP. Low PKA activity (or at least low cAMP) biases MSNs towards LTD. Testing of this hypothesis awaits future experiments. In the meantime, however, it also begs the question: what are the targets of PKA at excitatory synapses onto MSNs? Here, I outline how could PKA modulates mGluR signaling to regulate LTD. However, the targets of PKA that could modulate LTP are not known. One possibility is that PKA phosphorylates NMDA receptors directly to activate them. Other possible targets include the striatal-enriched phosphatases STEP46 and STEP61, and DARPP-32, all of which are expressed by MSNs and contain known PKA phosphorylation sites (Kuroiwa et al., 2008; Paul et al., 2000). PKA phosphorylation causes DARPP-32 to inhibit PP1. Inhibition of PP1, in turn, increases the phosphorylation of NMDA and AMPA receptors, activating

them (Greengard et al., 1999). PKA phosphorylation, as well as inhibition of PP1, also regulates STEP activity. Postsynaptic STEP and DARPP-32 signaling might be especially important for LTP since LTP is postsynaptically expressed. In agreement with this view, a mutant substrate-trapping form of STEP prevents LTP but not LTD (Tashev et al., 2009) and the loss of DARPP-32 prevents LTP in both direct- and indirect-pathway MSNs (Bateup et al.).

The issue of whether LTD and LTP are mechanistically linked also raises another critical unanswered question in the field. How can LTD and LTP act as opponent processes if the former is expressed presynaptically while the latter is expressed postsynaptically? By undergoing LTD, and then later LTP, a MSN synapse would not return to its original state, but would end up with a low presynaptic release probability but a robust ability to detect and respond to release events postsynaptically. Do all MSN excitatory synapses eventually become “locked” in this state? If so, synaptogenesis would be required to support continued plasticity (and, presumably, motor learning) in adulthood and the hypothesis put forth in the previous section would be invalid. Alternatively, there might be homeostatic resetting mechanisms for MSN synaptic strength. Such resetting mechanisms might be active – de-potentiation/de-depression mechanisms – or passive – slow resetting caused by constant cycling of cellular components. De-potentiation of MSN synapses has been observed using low-frequency stimulation (1-2 Hz) and involves apparently postsynaptic mechanisms including signaling by DARPP-32, PP1 and STEP (Centonze et al., 2006; Flajolet et al., 2008; Picconi et al., 2003; Tashev et al., 2009). De-depression of endocannabinoid-mediated LTD has not, to our knowledge, been demonstrated. Evidence for passive resetting of MSN synaptic strength is also scant, but passive resetting cannot yet be excluded as a possibility. The solution to the question of how MSNs maintain their ability to undergo

plasticity will be critical to our understanding of how the basal ganglia support action selection and learning processes.

How does striatal plasticity regulate motor behavior?

In the abstract for this thesis, I state that striatal plasticity "has the potential to powerfully regulate motor function by setting the gain on the incoming cortical signals that drive basal ganglia circuits." However, it remains unclear what exactly this gain modulation would do to basal ganglia circuit function and, by extension, motor output. The RGS4$^{-/-}$ mice I examine in Chapter 3, offer some interesting clues. Unilaterally dopamine-depleted RGS4$^{-/-}$ mice move more and are better coordinated than unilaterally dopamine-depleted wildtype mice, yet they still display an ipsilateral rotational bias. This finding suggests that striatal plasticity has more to do with fine-tuning circuits to coordinate complicated motor sequences than it does with gross motor functions. *In vivo* recordings from dopamine-depleted RGS4$^{-/-}$ mice could be an illuminating way to look at the circuit effects of RGS4 deficiency following dopamine depletion. Indeed, many future experiments will be required to clearly link specific forms of striatal plasticity to particular aspects of motor behavior. Hopefully, unraveling the mechanisms of at least one form of striatal plasticity has given future researchers some knowledge that will help them to make specific *in vivo* manipulations addressing this important question.

References

Ade, K.K., and Lovinger, D.M. (2007). Anandamide regulates postnatal development of long-term synaptic plasticity in the rat dorsolateral striatum. J Neurosci *27*, 2403-2409.

Adermark, L., and Lovinger, D.M. (2007). Combined activation of L-type Ca2+ channels and synaptic transmission is sufficient to induce striatal long-term depression. J Neurosci *27*, 6781-6787.

Ahn, K., McKinney, M.K., and Cravatt, B.F. (2008). Enzymatic pathways that regulate endocannabinoid signaling in the nervous system. Chemical reviews *108*, 1687-1707.

Albin, R.L., Young, A.B., and Penney, J.B. (1989). The functional anatomy of basal ganglia disorders. Trends in neurosciences *12*, 366-375.

Barraco, R.A., Martens, K.A., Parizon, M., and Normile, H.J. (1993). Adenosine A2a receptors in the nucleus accumbens mediate locomotor depression. Brain research bulletin *31*, 397-404.

Bateup, H.S., Santini, E., Shen, W., Birnbaum, S., Valjent, E., Surmeier, D.J., Fisone, G., Nestler, E.J., and Greengard, P. Distinct subclasses of medium spiny neurons differentially regulate striatal motor behaviors. Proceedings of the National Academy of Sciences of the United States of America *107*, 14845-14850.

Bence-Hanulec, K.K., Marshall, J., and Blair, L.A. (2000). Potentiation of neuronal L calcium channels by IGF-1 requires phosphorylation of the alpha1 subunit on a specific tyrosine residue. Neuron *27*, 121-131.

Bence, K., Ma, W., Kozasa, T., and Huang, X.Y. (1997). Direct stimulation of Bruton's tyrosine kinase by G(q)-protein alpha-subunit. Nature *389*, 296-299.

Blazer, L.L., Roman, D.L., Chung, A., Larsen, M.J., Greedy, B.M., Husbands, S.M., and Neubig, R.R. (2010). Reversible, allosteric small-molecule inhibitors of regulator of G protein signaling proteins. Molecular pharmacology *78*, 524-533.

Blazer, L.L., Zhang, H., Casey, E.M., Husbands, S.M., and Neubig, R.R. (2011). A nanomolar-potency small molecule inhibitor of regulator of g-protein signaling proteins. Biochemistry *50*, 3181-3192.

Bolam, J.P., Hanley, J.J., Booth, P.A., and Bevan, M.D. (2000). Synaptic organisation of the basal ganglia. J Anat *196 (Pt 4)*, 527-542.

Calabresi, P., Maj, R., Pisani, A., Mercuri, N.B., and Bernardi, G. (1992a). Long-term synaptic depression in the striatum: physiological and pharmacological characterization. J Neurosci *12*, 4224-4233.

Calabresi, P., Pisani, A., Mercuri, N.B., and Bernardi, G. (1992b). Long-term Potentiation in the Striatum is Unmasked by Removing the Voltage-dependent Magnesium Block of NMDA Receptor Channels. The European journal of neuroscience *4*, 929-935.

Calabresi, P., Pisani, A., Mercuri, N.B., and Bernardi, G. (1994). Post-receptor mechanisms underlying striatal long-term depression. J Neurosci *14*, 4871-4881.

Calabresi, P., Saiardi, A., Pisani, A., Baik, J.H., Centonze, D., Mercuri, N.B., Bernardi, G., and Borrelli, E. (1997). Abnormal synaptic plasticity in the striatum of mice lacking dopamine D2 receptors. J Neurosci *17*, 4536-4544.

Cechova, S., and Venton, B.J. (2008). Transient adenosine efflux in the rat caudate-putamen. Journal of neurochemistry *105*, 1253-1263.

Centonze, D., Costa, C., Rossi, S., Prosperetti, C., Pisani, A., Usiello, A., Bernardi, G., Mercuri, N.B., and Calabresi, P. (2006). Chronic cocaine prevents depotentiation at corticostriatal synapses. Biological psychiatry *60*, 436-443.

Chavis, P., Fagni, L., Lansman, J.B., and Bockaert, J. (1996). Functional coupling between ryanodine receptors and L-type calcium channels in neurons. Nature *382*, 719-722.

Chevaleyre, V., Takahashi, K.A., and Castillo, P.E. (2006). Endocannabinoid-mediated synaptic plasticity in the CNS. Annual review of neuroscience *29*, 37-76.

Choi, S., and Lovinger, D.M. (1997). Decreased probability of neurotransmitter release underlies striatal long-term depression and postnatal development of corticostriatal synapses. Proceedings of the National Academy of Sciences of the United States of America *94*, 2665-2670.

Dang, M.T., Yokoi, F., Yin, H.H., Lovinger, D.M., Wang, Y., and Li, Y. (2006). Disrupted motor learning and long-term synaptic plasticity in mice lacking NMDAR1 in the striatum. Proceedings of the National Academy of Sciences of the United States of America *103*, 15254-15259.

Day, M., Wokosin, D., Plotkin, J.L., Tian, X., and Surmeier, D.J. (2008). Differential excitability and modulation of striatal medium spiny neuron dendrites. J Neurosci *28*, 11603-11614.

DeLong, M., and Wichmann, T. (2009). Update on models of basal ganglia function and dysfunction. Parkinsonism & related disorders *15 Suppl 3*, S237-240.

DeLong, M.R. (1990). Primate models of movement disorders of basal ganglia origin. Trends in neurosciences *13*, 281-285.

DeLong, M.R., and Wichmann, T. (2007). Circuits and circuit disorders of the basal ganglia. Arch Neurol *64*, 20-24.

Ding, J., Guzman, J.N., Tkatch, T., Chen, S., Goldberg, J.A., Ebert, P.J., Levitt, P., Wilson, C.J., Hamm, H.E., and Surmeier, D.J. (2006). RGS4-dependent attenuation of M4 autoreceptor function in striatal cholinergic interneurons following dopamine depletion. Nature neuroscience *9*, 832-842.

Ding, J., Peterson, J.D., and Surmeier, D.J. (2008). Corticostriatal and thalamostriatal synapses have distinctive properties. J Neurosci *28*, 6483-6492.

Durieux, P.F., Bearzatto, B., Guiducci, S., Buch, T., Waisman, A., Zoli, M., Schiffmann, S.N., and de Kerchove d'Exaerde, A. (2009). D2R striatopallidal neurons inhibit both locomotor and drug reward processes. Nature neuroscience *12*, 393-395.

Engler, B., Freiman, I., Urbanski, M., and Szabo, B. (2006). Effects of exogenous and endogenous cannabinoids on GABAergic neurotransmission between the caudate-putamen and the globus pallidus in the mouse. The Journal of pharmacology and experimental therapeutics *316*, 608-617.

Ferre, S., Fredholm, B.B., Morelli, M., Popoli, P., and Fuxe, K. (1997). Adenosine-dopamine receptor-receptor interactions as an integrative mechanism in the basal ganglia. Trends in neurosciences *20*, 482-487.

Filion, M., and Tremblay, L. (1991). Abnormal spontaneous activity of globus pallidus neurons in monkeys with MPTP-induced parkinsonism. Brain research *547*, 142-151.

Fino, E., Glowinski, J., and Venance, L. (2005). Bidirectional activity-dependent plasticity at corticostriatal synapses. J Neurosci *25*, 11279-11287.

Fino, E., Paille, V., Cui, Y., Morera-Herreras, T., Deniau, J.M., and Venance, L. (2010). Distinct coincidence detectors govern the corticostriatal spike timing-dependent plasticity. The Journal of physiology *588*, 3045-3062.

Flajolet, M., Wang, Z., Futter, M., Shen, W., Nuangchamnong, N., Bendor, J., Wallach, I., Nairn, A.C., Surmeier, D.J., and Greengard, P. (2008). FGF acts as a co-transmitter through adenosine A(2A) receptor to regulate synaptic plasticity. Nature neuroscience *11*, 1402-1409.

Fuxe, K., Ferre, S., Canals, M., Torvinen, M., Terasmaa, A., Marcellino, D., Goldberg, S.R., Staines, W., Jacobsen, K.X., Lluis, C.*, et al.* (2005). Adenosine A2A and dopamine D2 heteromeric receptor complexes and their function. J Mol Neurosci *26*, 209-220.

Fuxe, K., Marcellino, D., Genedani, S., and Agnati, L. (2007). Adenosine A(2A) receptors, dopamine D(2) receptors and their interactions in Parkinson's disease. Mov Disord *22*, 1990-2017.

Gao, Y., Vasilyev, D.V., Goncalves, M.B., Howell, F.V., Hobbs, C., Reisenberg, M., Shen, R., Zhang, M.Y., Strassle, B.W., Lu, P.*, et al.* (2010). Loss of retrograde endocannabinoid signaling and reduced adult neurogenesis in diacylglycerol lipase knock-out mice. J Neurosci *30*, 2017-2024.

Gerdeman, G.L., Ronesi, J., and Lovinger, D.M. (2002). Postsynaptic endocannabinoid release is critical to long-term depression in the striatum. Nature neuroscience *5*, 446-451.

Gerfen, C.R., Engber, T.M., Mahan, L.C., Susel, Z., Chase, T.N., Monsma, F.J., Jr., and Sibley, D.R. (1990). D1 and D2 dopamine receptor-regulated gene expression of striatonigral and striatopallidal neurons. Science (New York, N.Y *250*, 1429-1432.

Gertler, T.S., Chan, C.S., and Surmeier, D.J. (2008). Dichotomous anatomical properties of adult striatal medium spiny neurons. J Neurosci *28*, 10814-10824.

Geurts, M., Maloteaux, J.M., and Hermans, E. (2003). Altered expression of regulators of G-protein signaling (RGS) mRNAs in the striatum of rats undergoing dopamine depletion. Biochemical pharmacology *66*, 1163-1170.

Giuffrida, A., Parsons, L.H., Kerr, T.M., Rodriguez de Fonseca, F., Navarro, M., and Piomelli, D. (1999). Dopamine activation of endogenous cannabinoid signaling in dorsal striatum. Nature neuroscience *2*, 358-363.

Gold, S.J., Ni, Y.G., Dohlman, H.G., and Nestler, E.J. (1997). Regulators of G-protein signaling (RGS) proteins: region-specific expression of nine subtypes in rat brain. J Neurosci *17*, 8024-8037.

Gong, S., Zheng, C., Doughty, M.L., Losos, K., Didkovsky, N., Schambra, U.B., Nowak, N.J., Joyner, A., Leblanc, G., Hatten, M.E., and Heintz, N. (2003). A gene expression atlas of the central nervous system based on bacterial artificial chromosomes. Nature *425*, 917-925.

Graybiel, A.M., Aosaki, T., Flaherty, A.W., and Kimura, M. (1994). The basal ganglia and adaptive motor control. Science (New York, N.Y *265*, 1826-1831.

Greengard, P., Allen, P.B., and Nairn, A.C. (1999). Beyond the dopamine receptor: the DARPP-32/protein phosphatase-1 cascade. Neuron *23*, 435-447.

Grillet, N., Pattyn, A., Contet, C., Kieffer, B.L., Goridis, C., and Brunet, J.F. (2005). Generation and characterization of Rgs4 mutant mice. Molecular and cellular biology *25*, 4221-4228.

Hansen, H.H., Schmid, P.C., Bittigau, P., Lastres-Becker, I., Berrendero, F., Manzanares, J., Ikonomidou, C., Schmid, H.H., Fernandez-Ruiz, J.J., and Hansen, H.S. (2001). Anandamide, but not 2-arachidonoylglycerol, accumulates during in vivo neurodegeneration. Journal of neurochemistry *78*, 1415-1427.

Hashimotodani, Y., Ohno-Shosaku, T., Tsubokawa, H., Ogata, H., Emoto, K., Maejima, T., Araishi, K., Shin, H.S., and Kano, M. (2005). Phospholipase Cbeta serves as a coincidence detector through its Ca2+ dependency for triggering retrograde endocannabinoid signal. Neuron *45*, 257-268.

Hauber, W., and Munkle, M. (1997). Motor depressant effects mediated by dopamine D2 and adenosine A2A receptors in the nucleus accumbens and the caudate-putamen. European journal of pharmacology *323*, 127-131.

Hauber, W., Nagel, J., Sauer, R., and Muller, C.E. (1998). Motor effects induced by a blockade of adenosine A2A receptors in the caudate-putamen. Neuroreport *9*, 1803-1806.

Henkels, K.M., Peng, H.J., Frondorf, K., and Gomez-Cambronero, J. (2010). A comprehensive model that explains the regulation of phospholipase D2 activity by phosphorylation-dephosphorylation. Molecular and cellular biology *30*, 2251-2263.

Higley, M.J., and Sabatini, B.L. (2010). Competitive regulation of synaptic Ca2+ influx by D2 dopamine and A2A adenosine receptors. Nature neuroscience *13*, 958-966.

Hikosaka, O., Takikawa, Y., and Kawagoe, R. (2000). Role of the basal ganglia in the control of purposive saccadic eye movements. Physiological reviews *80*, 953-978.

Huang, J., Zhou, H., Mahavadi, S., Sriwai, W., and Murthy, K.S. (2007). Inhibition of Galphaq-dependent PLC-beta1 activity by PKG and PKA is mediated by phosphorylation of RGS4 and GRK2. American journal of physiology *292*, C200-208.

Huang, Z.L., Qu, W.M., Eguchi, N., Chen, J.F., Schwarzschild, M.A., Fredholm, B.B., Urade, Y., and Hayaishi, O. (2005). Adenosine A2A, but not A1, receptors mediate the arousal effect of caffeine. Nature neuroscience *8*, 858-859.

Hubbard, K.B., and Hepler, J.R. (2006). Cell signalling diversity of the Gqalpha family of heterotrimeric G proteins. Cellular signalling *18*, 135-150.

Jenner, P., Mori, A., Hauser, R., Morelli, M., Fredholm, B.B., and Chen, J.F. (2009). Adenosine, adenosine A 2A antagonists, and Parkinson's disease. Parkinsonism & related disorders *15*, 406-413.

Jeon, J., Dencker, D., Wortwein, G., Woldbye, D.P., Cui, Y., Davis, A.A., Levey, A.I., Schutz, G., Sager, T.N., Mork, A*., et al.* (2010). A subpopulation of neuronal M4 muscarinic acetylcholine receptors plays a critical role in modulating dopamine-dependent behaviors. J Neurosci *30*, 2396-2405.

Jia, Y., Gall, C.M., and Lynch, G. (2010). Presynaptic BDNF promotes postsynaptic long-term potentiation in the dorsal striatum. J Neurosci *30*, 14440-14445.

Jung, K.M., Mangieri, R., Stapleton, C., Kim, J., Fegley, D., Wallace, M., Mackie, K., and Piomelli, D. (2005). Stimulation of endocannabinoid formation in brain slice cultures through activation of group I metabotropic glutamate receptors. Molecular pharmacology *68*, 1196-1202.

Kano, M., Ohno-Shosaku, T., Hashimotodani, Y., Uchigashima, M., and Watanabe, M. (2009). Endocannabinoid-mediated control of synaptic transmission. Physiological reviews *89*, 309-380.

Kerr, J.N., and Wickens, J.R. (2001). Dopamine D-1/D-5 receptor activation is required for long-term potentiation in the rat neostriatum in vitro. Journal of neurophysiology *85*, 117-124.

Kheirbek, M.A., Britt, J.P., Beeler, J.A., Ishikawa, Y., McGehee, D.S., and Zhuang, X. (2009). Adenylyl cyclase type 5 contributes to corticostriatal plasticity and striatum-dependent learning. J Neurosci *29*, 12115-12124.

Kim, D.S., and Palmiter, R.D. (2008). Interaction of dopamine and adenosine receptor function in behavior: studies with dopamine-deficient mice. Front Biosci *13*, 2311-2318.

Kitada, T., Pisani, A., Karouani, M., Haburcak, M., Martella, G., Tscherter, A., Platania, P., Wu, B., Pothos, E.N., and Shen, J. (2009). Impaired dopamine release and synaptic plasticity in the striatum of parkin-/- mice. Journal of neurochemistry *110*, 613-621.

Kitada, T., Pisani, A., Porter, D.R., Yamaguchi, H., Tscherter, A., Martella, G., Bonsi, P., Zhang, C., Pothos, E.N., and Shen, J. (2007). Impaired dopamine release and synaptic plasticity in the striatum of PINK1-deficient mice. Proceedings of the National Academy of Sciences of the United States of America *104*, 11441-11446.

Kravitz, A.V., Freeze, B.S., Parker, P.R.L., Kay, K., Thwin, M.T., Deisseroth, K., and Kreitzer, A.C. (2010). Regulation of parkinsonian motor behaviours by optogenetic control of basal ganglia circuitry. Nature *466*, 622-626.

Kreitzer, A.C., and Malenka, R.C. (2005). Dopamine modulation of state-dependent endocannabinoid release and long-term depression in the striatum. J Neurosci *25*, 10537-10545.

Kreitzer, A.C., and Malenka, R.C. (2007). Endocannabinoid-mediated rescue of striatal LTD and motor deficits in Parkinson's disease models. Nature *445*, 643-647.

Kreitzer, A.C., and Malenka, R.C. (2008). Striatal plasticity and basal ganglia circuit function. Neuron *60*, 543-554.

Kuhn, A., Goldstein, D.R., Hodges, A., Strand, A.D., Sengstag, T., Kooperberg, C., Becanovic, K., Pouladi, M.A., Sathasivam, K., Cha, J.H.*, et al.* (2007). Mutant huntingtin's effects on striatal gene expression in mice recapitulate changes observed in human Huntington's disease brain and do not differ with mutant huntingtin length or wild-type huntingtin dosage. Human molecular genetics *16*, 1845-1861.

Kuroiwa, M., Bateup, H.S., Shuto, T., Higashi, H., Tanaka, M., and Nishi, A. (2008). Regulation of DARPP-32 phosphorylation by three distinct dopamine D1-like receptor signaling pathways in the neostriatum. Journal of neurochemistry *107*, 1014-1026.

Kurz, A., Double, K.L., Lastres-Becker, I., Tozzi, A., Tantucci, M., Bockhart, V., Bonin, M., Garcia-Arencibia, M., Nuber, S., Schlaudraff, F.*, et al.* (2010). A53T-alpha-synuclein overexpression impairs dopamine signaling and striatal synaptic plasticity in old mice. PloS one *5*, e11464.

Lerner, T.N., Horne, E.A., Stella, N., and Kreitzer, A.C. (2010). Endocannabinoid signaling mediates psychomotor activation by adenosine A2A antagonists. J Neurosci *30*, 2160-2164.

Lerner, T.N., and Kreitzer, A.C. (2011). Neuromodulatory control of striatal plasticity and behavior. Current opinion in neurobiology.

Leung, D., Saghatelian, A., Simon, G.M., and Cravatt, B.F. (2006). Inactivation of N-acyl phosphatidylethanolamine phospholipase D reveals multiple mechanisms for the biosynthesis of endocannabinoids. Biochemistry *45*, 4720-4726.

Maccarrone, M., Rossi, S., Bari, M., De Chiara, V., Fezza, F., Musella, A., Gasperi, V., Prosperetti, C., Bernardi, G., Finazzi-Agro, A.*, et al.* (2008). Anandamide inhibits metabolism and physiological actions of 2-arachidonoylglycerol in the striatum. Nature neuroscience *11*, 152-159.

Marsicano, G., Wotjak, C.T., Azad, S.C., Bisogno, T., Rammes, G., Cascio, M.G., Hermann, H., Tang, J., Hofmann, C., Zieglgansberger, W., *et al.* (2002). The endogenous cannabinoid system controls extinction of aversive memories. Nature *418*, 530-534.

Mingote, S., Font, L., Farrar, A.M., Vontell, R., Worden, L.T., Stopper, C.M., Port, R.G., Sink, K.S., Bunce, J.G., Chrobak, J.J., and Salamone, J.D. (2008). Nucleus accumbens adenosine A2A receptors regulate exertion of effort by acting on the ventral striatopallidal pathway. J Neurosci *28*, 9037-9046.

Murthy, V.N., and Fetz, E.E. (1992). Coherent 25- to 35-Hz oscillations in the sensorimotor cortex of awake behaving monkeys. Proceedings of the National Academy of Sciences of the United States of America *89*, 5670-5674.

Narushima, M., Hashimoto, K., and Kano, M. (2006a). Endocannabinoid-mediated short-term suppression of excitatory synaptic transmission to medium spiny neurons in the striatum. Neuroscience research *54*, 159-164.

Narushima, M., Uchigashima, M., Hashimoto, K., Watanabe, M., and Kano, M. (2006b). Depolarization-induced suppression of inhibition mediated by endocannabinoids at synapses from fast-spiking interneurons to medium spiny neurons in the striatum. The European journal of neuroscience *24*, 2246-2252.

Nishi, A., Kuroiwa, M., Miller, D.B., O'Callaghan, J.P., Bateup, H.S., Shuto, T., Sotogaku, N., Fukuda, T., Heintz, N., Greengard, P., and Snyder, G.L. (2008). Distinct roles of PDE4 and PDE10A in the regulation of cAMP/PKA signaling in the striatum. J Neurosci *28*, 10460-10471.

Obeso, J.A., Rodriguez-Oroz, M.C., Rodriguez, M., Macias, R., Alvarez, L., Guridi, J., Vitek, J., and DeLong, M.R. (2000). Pathophysiologic basis of surgery for Parkinson's disease. Neurology *55*, S7-12.

Pacey, L.K., Doss, L., Cifelli, C., van der Kooy, D., Heximer, S.P., and Hampson, D.R. (2011). Genetic deletion of regulator of G-protein signaling 4 (RGS4) rescues a subset of fragile X related phenotypes in the FMR1 knockout mouse. Molecular and cellular neurosciences *46*, 563-572.

Packard, M.G., and Knowlton, B.J. (2002). Learning and memory functions of the Basal Ganglia. Annual review of neuroscience *25*, 563-593.

Paul, S., Snyder, G.L., Yokakura, H., Picciotto, M.R., Nairn, A.C., and Lombroso, P.J. (2000). The Dopamine/D1 receptor mediates the phosphorylation and inactivation of the protein tyrosine phosphatase STEP via a PKA-dependent pathway. J Neurosci *20*, 5630-5638.

Peterson, D.A., Sejnowski, T.J., and Poizner, H. (2010). Convergent evidence for abnormal striatal synaptic plasticity in dystonia. Neurobiology of disease *37*, 558-573.

Picconi, B., Centonze, D., Hakansson, K., Bernardi, G., Greengard, P., Fisone, G., Cenci, M.A., and Calabresi, P. (2003). Loss of bidirectional striatal synaptic plasticity in L-DOPA-induced dyskinesia. Nature neuroscience *6*, 501-506.

Piomelli, D. (2003). The molecular logic of endocannabinoid signalling. Nature reviews *4*, 873-884.

Ronesi, J., and Lovinger, D.M. (2005). Induction of striatal long-term synaptic depression by moderate frequency activation of cortical afferents in rat. The Journal of physiology *562*, 245-256.

Rosin, D.L., Hettinger, B.D., Lee, A., and Linden, J. (2003). Anatomy of adenosine A2A receptors in brain: morphological substrates for integration of striatal function. Neurology *61*, S12-18.

Rossi, S., Prosperetti, C., Picconi, B., De Chiara, V., Mataluni, G., Bernardi, G., Calabresi, P., and Centonze, D. (2006). Deficits of glutamate transmission in the striatum of toxic and genetic models of Huntington's disease. Neuroscience letters *410*, 6-10.

Saugstad, J.A., Marino, M.J., Folk, J.A., Hepler, J.R., and Conn, P.J. (1998). RGS4 inhibits signaling by group I metabotropic glutamate receptors. J Neurosci *18*, 905-913.

Schiffmann, S.N., Fisone, G., Moresco, R., Cunha, R.A., and Ferre, S. (2007). Adenosine A(2A) receptors and basal ganglia physiology. Progress in neurobiology.

Schiffmann, S.N., Jacobs, O., and Vanderhaeghen, J.J. (1991). Striatal restricted adenosine A2 receptor (RDC8) is expressed by enkephalin but not by substance P neurons: an in situ hybridization histochemistry study. Journal of neurochemistry *57*, 1062-1067.

Schwarzschild, M.A., Agnati, L., Fuxe, K., Chen, J.F., and Morelli, M. (2006). Targeting adenosine A2A receptors in Parkinson's disease. Trends in neurosciences *29*, 647-654.

Schwendt, M., Hearing, M.C., See, R.E., and McGinty, J.F. (2007). Chronic cocaine reduces RGS4 mRNA in rat prefrontal cortex and dorsal striatum. Neuroreport *18*, 1261-1265.

Schwendt, M., and McGinty, J.F. (2007). Regulator of G-protein signaling 4 interacts with metabotropic glutamate receptor subtype 5 in rat striatum: relevance to amphetamine behavioral sensitization. The Journal of pharmacology and experimental therapeutics *323*, 650-657.

Sebastiao, A.M., and Ribeiro, J.A. (1996). Adenosine A2 receptor-mediated excitatory actions on the nervous system. Progress in neurobiology *48*, 167-189.

Shen, H.Y., Coelho, J.E., Ohtsuka, N., Canas, P.M., Day, Y.J., Huang, Q.Y., Rebola, N., Yu, L., Boison, D., Cunha, R.A*., et al.* (2008a). A critical role of the adenosine A2A receptor in extrastriatal neurons in modulating psychomotor activity as revealed by opposite phenotypes of striatum and forebrain A2A receptor knock-outs. J Neurosci *28*, 2970-2975.

Shen, W., Flajolet, M., Greengard, P., and Surmeier, D.J. (2008b). Dichotomous dopaminergic control of striatal synaptic plasticity. Science (New York, N.Y *321*, 848-851.

Shen, W., Tian, X., Day, M., Ulrich, S., Tkatch, T., Nathanson, N.M., and Surmeier, D.J. (2007). Cholinergic modulation of Kir2 channels selectively elevates dendritic excitability in striatopallidal neurons. Nature neuroscience *10*, 1458-1466.

Shindou, T., Arbuthnott, G.W., and Wickens, J.R. (2008). Actions of adenosine A 2A receptors on synaptic connections of spiny projection neurons in the neostriatal inhibitory network. Journal of neurophysiology *99*, 1884-1889.

Shindou, T., Nonaka, H., Richardson, P.J., Mori, A., Kase, H., and Ichimura, M. (2002). Presynaptic adenosine A2A receptors enhance GABAergic synaptic transmission via a cyclic AMP dependent mechanism in the rat globus pallidus. British journal of pharmacology *136*, 296-302.

Shindou, T., Richardson, P.J., Mori, A., Kase, H., and Ichimura, M. (2003). Adenosine modulates the striatal GABAergic inputs to the globus pallidus via adenosine A2A receptors in rats. Neuroscience letters *352*, 167-170.

Shuen, J.A., Chen, M., Gloss, B., and Calakos, N. (2008). Drd1a-tdTomato BAC transgenic mice for simultaneous visualization of medium spiny neurons in the direct and indirect pathways of the basal ganglia. J Neurosci *28*, 2681-2685.

Simola, N., Morelli, M., and Pinna, A. (2008). Adenosine A2A receptor antagonists and Parkinson's disease: state of the art and future directions. Current pharmaceutical design *14*, 1475-1489.

Smith, Y., Bevan, M.D., Shink, E., and Bolam, J.P. (1998). Microcircuitry of the direct and indirect pathways of the basal ganglia. Neuroscience *86*, 353-387.

Steinmetz, P.N., Roy, A., Fitzgerald, P.J., Hsiao, S.S., Johnson, K.O., and Niebur, E. (2000). Attention modulates synchronized neuronal firing in primate somatosensory cortex. Nature *404*, 187-190.

Stromberg, I., Popoli, P., Muller, C.E., Ferre, S., and Fuxe, K. (2000). Electrophysiological and behavioural evidence for an antagonistic modulatory role of adenosine A2A receptors in dopamine D2 receptor regulation in the rat dopamine-denervated striatum. The European journal of neuroscience *12*, 4033-4037.

Sung, K.W., Choi, S., and Lovinger, D.M. (2001). Activation of group I mGluRs is necessary for induction of long-term depression at striatal synapses. Journal of neurophysiology *86*, 2405-2412.

Surmeier, D.J., Plotkin, J., and Shen, W. (2009). Dopamine and synaptic plasticity in dorsal striatal circuits controlling action selection. Current opinion in neurobiology *19*, 621-628.

Svenningsson, P., Nomikos, G.G., Ongini, E., and Fredholm, B.B. (1997). Antagonism of adenosine A2A receptors underlies the behavioural activating effect of caffeine and is associated with reduced expression of messenger RNA for NGFI-A and NGFI-B in caudate-putamen and nucleus accumbens. Neuroscience *79*, 753-764.

Tanimura, A., Yamazaki, M., Hashimotodani, Y., Uchigashima, M., Kawata, S., Abe, M., Kita, Y., Hashimoto, K., Shimizu, T., Watanabe, M.*, et al.* (2010). The endocannabinoid 2-arachidonoylglycerol produced by diacylglycerol lipase alpha mediates retrograde suppression of synaptic transmission. Neuron *65*, 320-327.

Tashev, R., Moura, P.J., Venkitaramani, D.V., Prosperetti, C., Centonze, D., Paul, S., and Lombroso, P.J. (2009). A substrate trapping mutant form of striatal-enriched protein tyrosine phosphatase prevents amphetamine-induced stereotypies and long-term potentiation in the striatum. Biological psychiatry *65*, 637-645.

Taverna, S., Ilijic, E., and Surmeier, D.J. (2008). Recurrent collateral connections of striatal medium spiny neurons are disrupted in models of Parkinson's disease. J Neurosci *28*, 5504-5512.

Taylor, S.J., Chae, H.Z., Rhee, S.G., and Exton, J.H. (1991). Activation of the beta 1 isozyme of phospholipase C by alpha subunits of the Gq class of G proteins. Nature *350*, 516-518.

Taymans, J.M., Kia, H.K., Claes, R., Cruz, C., Leysen, J., and Langlois, X. (2004). Dopamine receptor-mediated regulation of RGS2 and RGS4 mRNA differentially depends on ascending dopamine projections and time. The European journal of neuroscience *19*, 2249-2260.

Tozzi, A., de Iure, A., Di Filippo, M., Tantucci, M., Costa, C., Borsini, F., Ghiglieri, V., Giampa, C., Fusco, F.R., Picconi, B., and Calabresi, P. (2011). The distinct role of medium spiny neurons and cholinergic interneurons in the D2/A2A receptor interaction in the striatum: implications for Parkinson's disease. J Neurosci *31*, 1850-1862.

Tozzi, A., Tscherter, A., Belcastro, V., Tantucci, M., Costa, C., Picconi, B., Centonze, D., Calabresi, P., and Borsini, F. (2007). Interaction of A2A adenosine and D2 dopamine receptors modulates corticostriatal glutamatergic transmission. Neuropharmacology *53*, 783-789.

Turner, R.S., and Desmurget, M. (2010). Basal ganglia contributions to motor control: a vigorous tutor. Current opinion in neurobiology *20*, 704-716.

Uchigashima, M., Narushima, M., Fukaya, M., Katona, I., Kano, M., and Watanabe, M. (2007). Subcellular arrangement of molecules for 2-arachidonoyl-glycerol-mediated retrograde signaling and its physiological contribution to synaptic modulation in the striatum. J Neurosci *27*, 3663-3676.

Wang, Z., Kai, L., Day, M., Ronesi, J., Yin, H.H., Ding, J., Tkatch, T., Lovinger, D.M., and Surmeier, D.J. (2006). Dopaminergic control of corticostriatal long-term synaptic depression in medium spiny neurons is mediated by cholinergic interneurons. Neuron *50*, 443-452.

Wilson, C.J., and Kawaguchi, Y. (1996). The origins of two-state spontaneous membrane potential fluctuations of neostriatal spiny neurons. J Neurosci *16*, 2397-2410.

Yin, H.H., and Knowlton, B.J. (2006). The role of the basal ganglia in habit formation. Nature reviews *7*, 464-476.

Yin, H.H., and Lovinger, D.M. (2006). Frequency-specific and D2 receptor-mediated inhibition of glutamate release by retrograde endocannabinoid signaling. Proceedings of the National Academy of Sciences of the United States of America *103*, 8251-8256.

Yin, H.H., Mulcare, S.P., Hilario, M.R., Clouse, E., Holloway, T., Davis, M.I., Hansson, A.C., Lovinger, D.M., and Costa, R.M. (2009). Dynamic reorganization of striatal circuits during the acquisition and consolidation of a skill. Nature neuroscience *12*, 333-341.

Zhang, Y., James, M., Middleton, F.A., and Davis, R.L. (2005). Transcriptional analysis of multiple brain regions in Parkinson's disease supports the involvement of specific protein processing, energy metabolism, and signaling pathways, and suggests novel disease mechanisms. Am J Med Genet B Neuropsychiatr Genet *137B*, 5-16.

Publishing Agreement

It is the policy of the University to encourage the distribution of all theses, dissertations, and manuscripts. Copies of all UCSF theses, dissertations, and manuscripts will be routed to the library via the Graduate Division. The library will make all theses, dissertations, and manuscripts accessible to the public and will preserve these to the best of their abilities, in perpetuity.

Please sign the following statement:

I hereby grant permission to the Graduate Division of the University of California, San Francisco to release copies of my thesis, dissertation, or manuscript to the Campus Library to provide access and preservation, in whole or in part, in perpetuity.

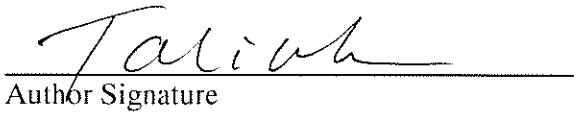

Author Signature

12/16/11

Date